How Stable Are Single-Cell Embeddings? A Comprehensive Analysis of Dimensionality Reduction Under Input Shuffling

Yu-Ting Huang[1] and *Jia-Ming* Chang[1,2*]

[1]Department of Computer Science, National Chengchi University, Taipei, Taiwan
[2]Institute of Neuroscience, National Chengchi University, Taipei, Taiwan

Abstract. Single-cell RNA sequencing (scRNA-seq) offers precise quantification of the transcriptome at an individual cell level, surpassing traditional bulk RNA-seq. Despite its advancements, the high-dimensional nature of scRNA-seq data complicates the extraction and visualization of underlying biological information. Various dimensionality reduction algorithms have been developed to aid biologists in uncovering cellular relationships, especially through clustering. However, the stability of single-cell dimensionality reduction has been largely overlooked, particularly the variation of neighbor relations or cluster quality in the reduced space.

In this study, we generate alternative datasets by randomly shuffling rows or columns of the single-cell expression matrix. These alternative datasets are processed similarly to the original data. Stability is measured by comparing results from the original and alternative data using multiple metrics, including *knn*-preservation for neighbor relations, the Calinski-Harabasz, Davies-Bouldin, and Xie-Beni indexes for cluster internal evaluation, and the Jaccard Index for clustering consistency. Additionally, the RF-hierarchical metric evaluated the preservation of global meta-information.

We employed Monocle 3, an *R* toolkit, to assess the stability of scRNA-seq visualizations using two popular methods: t-SNE and UMAP. Our evaluation involved six datasets, including two from the C. elegans Monocle 3 tutorial, two from the Single Cell Portal (PBMC ID 345 and islet ID 1526), and two comprising Mouse Retinal and Brain samples. Internal cluster scores varied after data shuffling, with the Jaccard Index of C. elegans-con dropping below 0.6, indicating instability, and the RF distance of SCP1526 reaching the maximum value. Our findings suggest that dimensionality reduction techniques vary in stability with shuffled inputs, indicating that claims of their robustness may be premature without considering input variations.

1 Introduction

* Corresponding author: chang.jiaming@gmail.com

1.1 Single-Cell RNA-Seq: Data Generation and Analysis

Single-cell RNA sequencing (scRNA-seq) revolutionizes our understanding of cellular diversity by enabling precise quantification of transcriptomes at the individual cell level, a significant leap over traditional bulk RNA-seq. Among the various platforms for generating scRNA-seq data, 10x Chromium stands out as the most popular and significant. Developed by 10x Genomics, this platform utilizes millions of unique barcode sequences to label cells within gel beads. These beads are mixed with cells and enzymes, and through an oil droplet encapsulation process, gel bead-in-emulsions (GEMs) are formed. Within these GEMs, the gel beads dissolve, releasing barcode sequences that uniquely tag each cell's RNA, subsequently collected and constructed into a sequencing library.

The analytical capabilities of scRNA-seq extend far beyond distinguishing between healthy and cancerous cells, as with bulk RNA-seq. It allows researchers to discern molecular differences at a cellular resolution, potentially identifying unique cellular signatures within cancerous tissues. The standard scRNA-seq analysis workflow involves isolating cells from heterogeneous tissues, sequencing the RNA from each cell, and generating sparse matrices of gene expression. These matrices are then subjected to dimensionality reduction techniques, enabling biologists to perform deeper analyses, such as discovering new cell types and understanding cellular functions in unprecedented detail.

1.2 Single-Cell Data Visualization through Dimensionality reduction Techniques

The high dimensionality of single-cell data, often around 1000 dimensions, presents a challenge known as the curse of dimensionality, which complicates data analysis and visualization. Dimensionality reduction techniques are crucial as they simplify the high-dimensional data into 2D or 3D visual representations while preserving essential features and information. Among these techniques, Principal Component Analysis (PCA) is a widely used statistical method that transforms observations of potentially correlated variables into a set of linearly uncorrelated variables known as principal components through an orthogonal transformation.

In addition to PCA, several nonlinear methods have been developed to handle the complexities of single-cell data. We utilize two prominent nonlinear dimensionality reduction methods — t-SNE, and UMAP—to analyze stability in visualizing single-cell data. t-Distributed Stochastic Neighbor Embedding (t-SNE) focuses on maintaining local data relationships in low-dimensional space by modeling cell relationships with a t-distribution [1]. Unlike t-SNE, Uniform Manifold Approximation and Projection (UMAP) leverages theories from Riemannian geometry and algebraic topology, providing advantages in retaining global data structure, runtime efficiency, and scalability [2].

These methods are implemented using the Monocle 3 package [3], which offers functionalities for cell clustering, classification, and counting, aiding in the discovery of new cell types. Additionally, Monocle 3 supports the construction of single-cell trajectories and differential gene expression analysis, though our primary focus is on using its clustering and classification capabilities to assess the performance of t-SNE, and UMAP across various datasets.

1.3 Stability of Dimensionality reduction Techniques in Single-Cell Analysis

Dimensionality reduction techniques play a crucial role in single-cell analysis, prompting numerous studies to evaluate their stability. For instance, Tang, M. et al. utilized the Jaccard Index (JI) to assess the consistency of cluster identities before and after re-clustering,

comparing the similarity of clusters across different runs [4]. A high JI indicates that cell identities within a cluster are reliably preserved across random subsets and re-clustering attempts. Another key measure, *knn*-preservation, introduced by Heiser, CN. et al., evaluates the preservation of global and local structures across various dimensionality reduction methods [5]. Their findings highlighted that UMAP tends to compress small local distances more significantly than t-SNE, impacting the local structure preservation.

Further, Liu, X. et al. implemented three metrics—the Calinski-Harabasz index (CH), the Davies-Bouldin index (DB), and the Xie-Beni Index (XB)—to perform internal evaluations of clustering outcomes [6]. These indices quantify the quality of clusters based on compactness and separation, providing insights into the aggregate structural integrity of the dataset. These methodologies collectively contribute to a comprehensive assessment of the stability of dimensionality reduction techniques, crucial for ensuring the reliability of single-cell analyses.

1.4 Assessing the Stability of Dimensionality reduction in Response to Data Shuffling

Inspired by the findings of Chatzou, M. et al., who documented numerical instability in large-scale progressive multiple alignment methods when processing shuffled amino-acid sequences [7], we explored similar concepts in our study. Their research demonstrated that varying the input order of sequences led to significant discrepancies in output, including notable shifts in cluster locations across different phylogenetic trees. Motivated by this, we shuffled our input data matrices by rows (genes) or columns (cells) before conducting dimensionality reduction analyses on single-cell data.

This approach allowed us to investigate whether the dimensionality reduction outcomes varied with the shuffling of input data. To assess any changes in the cell-to-cell relationships post-shuffling, we employed *knn*-preservation as a key metric. Additionally, we utilized three internal evaluation indices — CH index, DB index, and XB index — to determine the quality of clustering. These indices measure the homogeneity within clusters and the heterogeneity between them, with higher values indicating better clustering quality.

Moreover, the JI was used to verify whether cells grouped in one set of results consistently clustered together in another set post-shuffling. Lastly, the Robinson-Foulds hierarchical (RF-hierarchical) metric was applied to measure the preservation of global structural integrity and the distances between clusters. These metrics collectively enabled us to comprehensively evaluate the stability of dimensionality reduction techniques in the face of shuffled data inputs.

2 Method

2.1 Dataset

Our study employs six datasets, each chosen to evaluate the stability of different dimensionality reduction techniques. Two originate from studies on C. elegans. The first of these, from Cao & Packer et al. [8], is a large dataset featuring over forty thousand cells and more than two thousand genes, representing differentiated cell types and highlighted in Figure 1 [8] as a discrete example. The second, from Packer & Zhu et al. [9], contains time-series data of whole developing embryos and predominantly neuronal cells, with 6,188 cells and over two thousand genes. This continuous dataset is challenging for clustering due to its focus on a single cell type. Both datasets are utilized in the Monocle 3 tutorial.

Additionally, we include four datasets from other sources for further testing. The first two are from the Single Cell Portal: one from human PBMCs (SCP345), derived from two healthy donors and comprising 13,316 cells and 21,844 genes; the other from stem cell-derived islet cells (SCP1526), featuring 46,261 cells and 20,621 genes, which includes cell development stage information [10]. The remaining two datasets are the Mouse Retina dataset [11], used as a benchmark in the study by Heiser CN. et al. [4], containing 6,600 cells and 20,478 genes, and the Mouse Brain dataset from Ximerakis M. et al. [11], which lacks specific cell type information, thus used solely for evaluating unsupervised clustering labels. The comprehensive details of these datasets are summarized in Table 1.

Table 1. The cells and genes count of the datasets used in our work.

Dataset	Meta Information	Cells	Genes
C. elegans-dis	cell type	42,035	20,271
C. elegans-con	cell type/time-series	6,188	20,222
SCP345	cell type	13,316	21,814
SCP1526	cell type/development stage	46,261	20,621
Mouse Retina	none	6,600	20,478
Mouse Brain	none	3,803	14,699

2.2 Shuffle test

We evaluate the stability of dimensionality reduction methods t-SNE, UMAP, and PCA using the Monocle 3 package, which is specifically designed for scRNA-seq data analysis, while the PHATE method is run using its dedicated Python package. Our experimental methodology comprises five key steps, as illustrated in Figure 1:

Step 1. Monocle 3 performs PCA during the preprocessing stage to simplify the high-dimensional scRNA-seq data before further analysis.

Step 2. We apply t-SNE, UMAP, and PCA for dimensionality reduction, projecting the data into 2D space for easier visualization and analysis.

Step 3. Using the Leiden algorithm, cells in the 2D space are grouped based on a community detection algorithm. Further, the Partition-based Graph Abstraction (PAGA) algorithm aggregates smaller clusters into larger partitions. Unlike clusters, partitions categorize cells into broader, more distinctly separated groups. If available, cell types are labeled based on dataset metadata for supervised analysis.

Step 4. We shuffle the input sparse matrix randomly by rows (genes) or columns (cells) to generate new inputs, naming gene-shuffled and cell-shuffled, respectively, as depicted by the blue arrow in Supplemental Figure 1. Subsequently, we reapply Steps 1 to 3 to re-cluster the cells. The shuffle process is conducted five times.

Step 5. We assess the stability of the dimensionality reduction techniques by calculating the JI, *knn*-preservation, CH, DB, XB, and the RF-hierarchical metric. It is important to note that RF-hierarchical can only be applied to data that includes cell type information for a supervised evaluation.

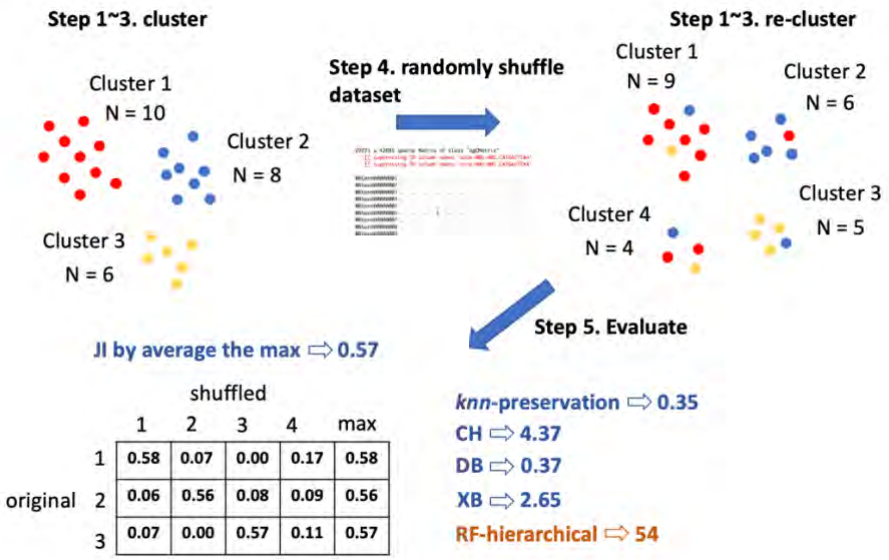

Fig. 1. The experiment workflow. First, we do the clustering (Steps 1~3), randomly shuffle the input sparse matrix (Step 4), then redo Steps 1~3. Finally, we calculate JI, *knn*-preservation, three internal indexes (CH, DB, XB) and RF-hierarchical in Step 5.

2.3 Stability Evaluation

Our evaluation of dimensionality reduction stability is categorized into two levels: *neighbor relations* or *cluster quality*.

2.3.1 Neighbor relations

One metric used is *knn*-preservation, which examines whether the neighbor relationships among cells are maintained after dimensionality reduction and subsequent shuffling. Additionally, the Robinson-Foulds (RF) distance, originally designed to assess the similarity of phylogenetic trees [12], is adapted here to evaluate the resemblance between hierarchical clustering outcomes of single-cell data metadata. In the context of scRNA-seq data visualization post-dimensionality reduction, the RF distance serves as a metric to compare the fidelity of cell-to-cell relationships before and after data manipulation.

2.3.1.1 knn-preservation

Building on the method introduced by Heiser CN. et al. [4], we calculate the k-nearest neighbors (*kNN*) for specific cells across different representations: native space (*kNN*-native), 2D plane (*kNN*-2D plane), and the shuffled 2D plane (shuffled *kNN*-2D plane). We define *kNN*-preservation by comparing the intersections of these neighbor sets using the following equation:

$$\frac{1}{nk}\sum_{i=1}^{n}|N_i \cap P_i|$$

, where n represents the number of cells analyzed, k indicates the number of nearest neighbors considered, Ni is the set of k-nearest neighbors of cell i in native space, Pi denotes the k-nearest neighbors in the 2D plane (or PSi for the shuffled 2D plane). To illustrate, Supplemental Figure 2 shows an example with $k = 3$ and $i = 1$ where the pink points represent the distribution of *knn*-native where cell 1's neighbors are cells 2, 3, and 4 ($N_1 = 2, 3, 4$). The green points represent cells in the *knn*-2D plane where $P_1 = 3, 5, 6$. The blue points represent cells in the shuffled *knn*-2D plane where $PS_1 = 2, 4, 6$. Then, *knn*-preservation between the native space and the 2D plane is 1/3; *knn*-preservation between the 2D space and the shuffled 2D plane is 2/3 for $i = 1$.

For the *C. elegans*-dis dataset, which contains 42,035 cells, the computational burden (e.g., a distance matrix of 42,035 x 42,035) necessitates subsampling for feasibility. In contrast, the *C. elegans*-con dataset with 6,188 cells allows for full dataset analysis without subsampling. The gene features, significant in both datasets (20,271 for *C. elegans*-dis and 20,222 for *C. elegans*-con), are refined using Seurat, which selects the top 500 variable genes based on a variance stabilizing transformation. This transformation stabilizes expression variance by correlating bead-level expression variance with mean expression.

2.3.1.2 RF-hierarchical

The definition of the global structure is the distance between clusters after making dimensionality reduction, i.e., the relationship with a pairwise cluster. First, we calculate each cell type's centroid to see the relationship between the cell type for each set. Second, we calculate the pairwise distance between each centroid. Finally, we generate a simple bottom-up hierarchical clustering by the UPGMA algorithm [13] to group the cell type based on the pairwise distance matrix. The stability of dimensionality reduction is quantified based on the topology similarity between the T_O (UPGMA tree of the original clustering) and T_S (UPGMA tree of the shuffled clustering). The Robinson-Foulds distance is the number of branches defined in T_O that do not have splits in T_S, plus the number of branches defined in T_S that do not have splits in T_O. Given unrooted n clusters, the range of Robinson-Foulds distance is from 0 (identical) to the worst case, $2n$-6. An example is given in Supplemental Figure 3 with the RF value 2.

2.3.2 Cluster quality

This involves assessing cluster labels of cells both before and after the shuffling process. Internal evaluation measures the effectiveness of unsupervised clustering by assessing the homogeneity within clusters and heterogeneity between them. We employ three internal evaluation indices: the CH, the DB, and the XB indexes. These indices assess the quality of clusters by measuring their compactness and separation. Another metric is the Jaccard Index (JI), which evaluates cluster stability by determining if cells that were grouped together pre-shuffling remain together post-shuffling.

2.3.2.1 Calinski-Harabasz index

The Calinski-Harabasz (CH) index applies two statistical indicators, Between-Group Sum of Squares (BGSS) and the Within-Group Sum of Squares (WGSS) [14]. BGSS measures the difference between each cluster's centroid (whole variance) and WGSS represents the differences within each cluster (local variance). Detail equations of the CH index is

summarized in Supplemental Section 1. So, a clustering should have the larger BGSS and the smaller WGSS. That is, the higher the CH score is, the better a clustering is.

2.3.2.2 Davies-Bouldin index

The Davies-Bouldin (DB) index is the average similarity between each cluster, a lower DB index is associated with a model with better separation between clusters [15]. Detail equations is summarized in Supplemental Section 2.

2.3.2.3 Xie-Beni Index

Xie-Beni (XB) index also uses the WGSS statistical indicator, which is used to be divided by the minimum of the least squared distance between points in the cluster [16]. By the formula of XB, the smaller the WGSS is, the smaller the XB is, and the better clustering is. Detail equations is summarized in Supplemental Section 3.

2.3.2.4 Jaccard Index

The JI is used to assess the similarity between clusters, particularly useful in our shuffling tests. It measures the overlap between two sets, A and B, where A is an original cluster and B is a cluster post-shuffling. The index represents the ratio of the intersection (common cells between A and B) to the union of the two clusters Detail equations is summarized in Supplemental Section 4. We use the maximum JI for each cluster and then compute the mean of these values to evaluate overall cluster stability. Stability thresholds are defined as follows: a JI below 0.60 indicates *instability*, between 0.60 and 0.75 suggests moderate *stability*, and above 0.85 signifies *high stability*.

3 Results

We assessed stability through both visualization and quantitative methods.

3.1 Visualization

After shuffling the input matrix, t-SNE and UMAP graphs remained largely similar to the originals, though subtle reorganizations of certain groups were observed. To better interpret these visual changes, we focused on the biological relationships among clusters rather than their absolute spatial positions, since distances in two-dimensional embeddings do not directly represent quantitative similarities.

3.1.1 C. elegans-dis

The *C. elegans-dis* dataset represents differentiated cell types at the organismal level. In the original t-SNE and UMAP embeddings (Figure 2, column a), cell types such as Coelomocytes, Hypodermal cells, and Neurons occupy distinct regions corresponding to their known developmental lineages. After shuffling, Coelomocytes appear repositioned relative to Hypodermal and Seam cell clusters (Figure 2, columns b–c). Although these shifts are not meaningful in absolute spatial terms, they indicate altered neighborhood relationships among biologically related cell types. Such changes suggest that the preservation of lineage-consistent proximity, important for interpreting differentiation trajectories, is sensitive to the ordering of input data. For example, Coelomocytes becoming separated from their expected

neighbors implies that data shuffling can disrupt biologically coherent grouping patterns, even when overall clustering structure remains visually intact.

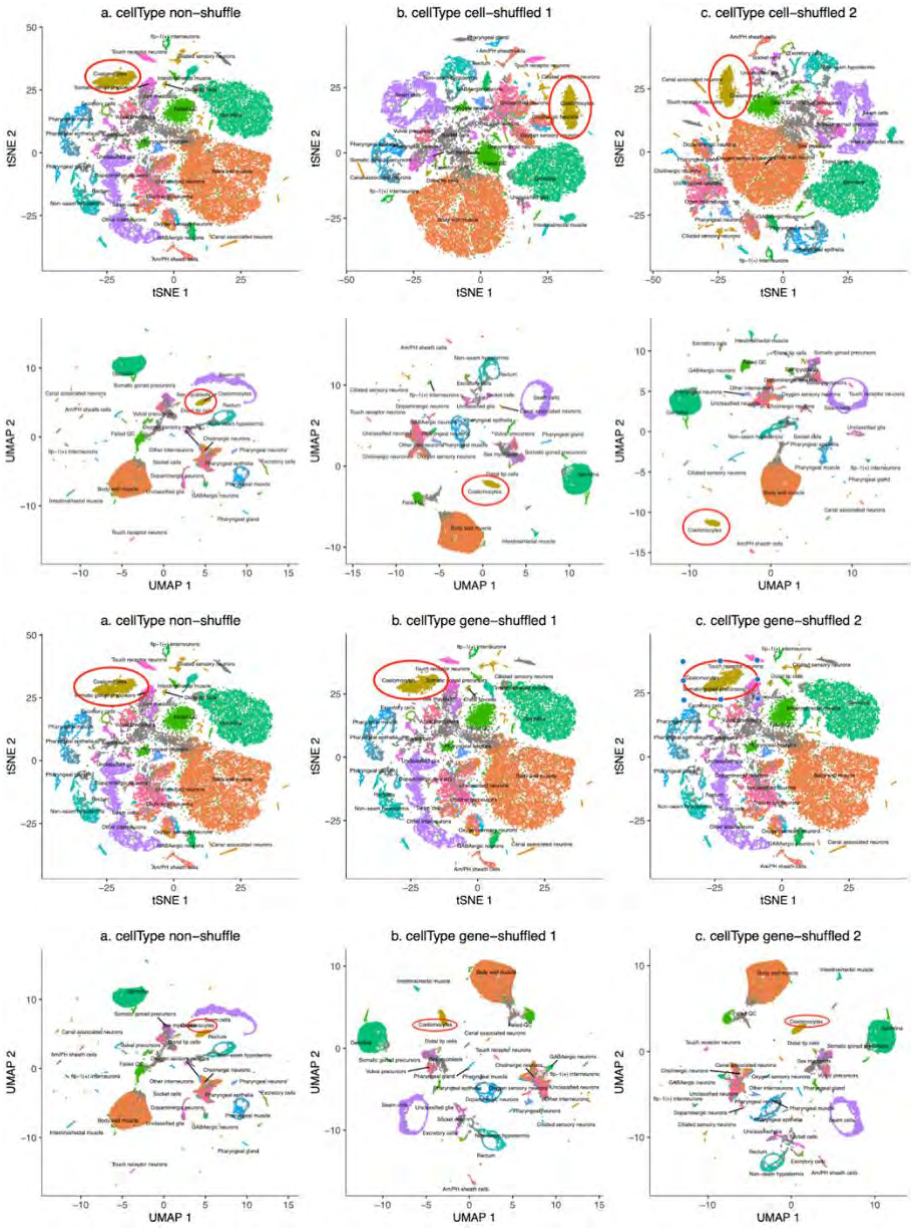

Fig. 2. Visualizations of *C. elegans*-dis by Monocle 3 are shown in sequences: original (column a), cell/gene-shuffled once (column b) and twice (column c) for t-SNE (the first and third rows) and UMAP (the second and fourth rows). These are labeled by Cao cell type with Coelomocytes highlighted in a red circle.

3.1.2 C. elegans-con

The *C. elegans-con* dataset captures embryonic development, where cells follow a continuous trajectory from progenitor to terminal states. In the UMAP visualization of the non-shuffled data (Figure 3, column a), the ASE parent cell type and its daughter subtypes ASER and ASEL are located in close proximity, consistent with their developmental lineage. After shuffling (Figure 3, columns b–c), ASER and ASEL become more distant from ASE and instead align closer to unrelated neuronal groups. This altered topological relationship affects biological interpretation: it may lead one to infer incorrect lineage continuity or misidentify differentiation branches. In contrast, the t-SNE representations tend to merge these subtypes across all conditions, showing less separation but also less sensitivity to the shuffling perturbation.

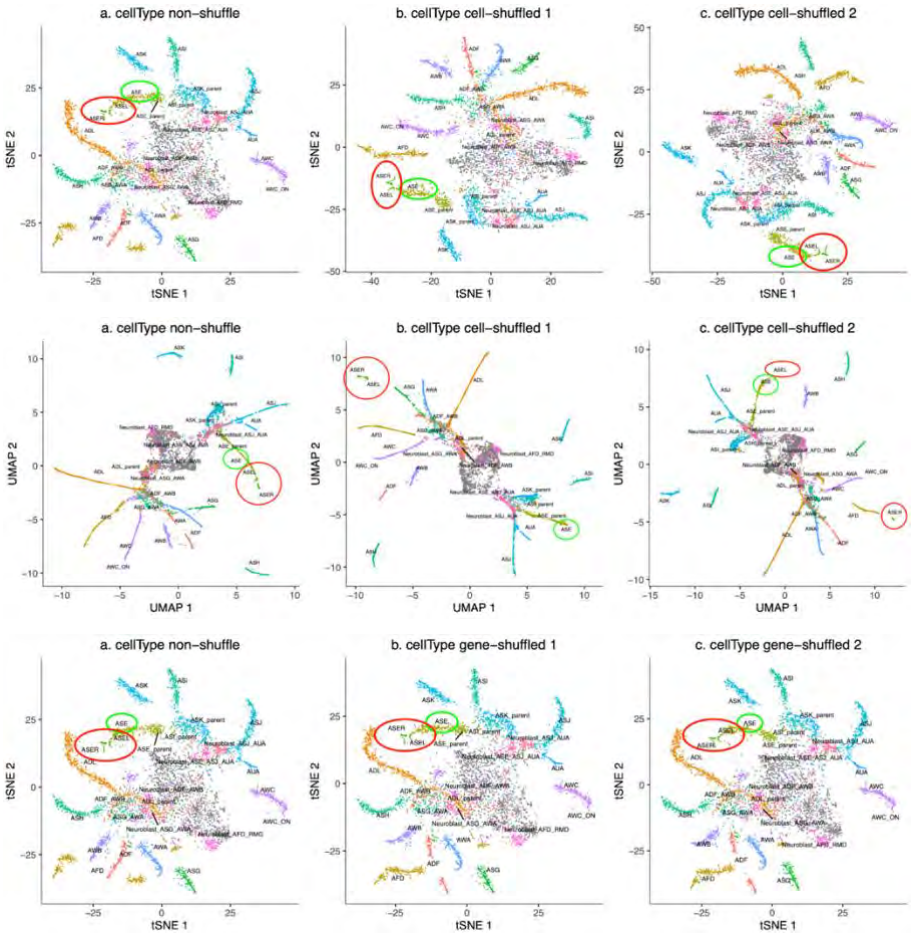

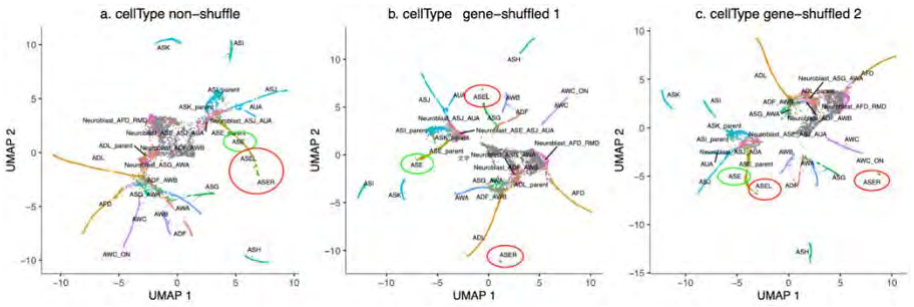

Fig. 3. Visualizations of *C. elegans*-con by Monocle 3 are shown in sequences: original (column a), cell/gene-shuffled once (column b) and twice (column c) for t-SNE (the first and third rows) and UMAP (the second and fourth rows). These are labelled by Cao cell type with ASER and ASEL highlighted in a red circle and ASE highlighted in green circle.

3.1.3 SCP345 and SCP1526

In the SCP345 dataset, the clustering of both cell-shuffled and gene-shuffled remains largely unchanged (Supplemental Figure 4), though slight variations in cluster shape and orientation are note. Supplemental Figure 5 shows the SCP1526 results for t-SNE and UMAP, with minimal changes beyond picture rotation.

3.1.4 Mouse Retina and Brain

Figure 4 displays the t-SNE and UMAP results for the Mouse Retina dataset after cell and gene shuffling. The non-shuffled data produces 12 clusters. Cell-shuffling reduces the cluster count, while gene-shuffling retains 12 clusters.

Supplemental Figure 6 show the t-SNE and UMAP results for the Mouse Brain dataset after cell and gene shuffling. The UMAP visualization of the Mouse Brain dataset under cell-shuffled conditions, resulting in a symmetric map. The UMAP visualization under gene-shuffled conditions appears more inconsistent.

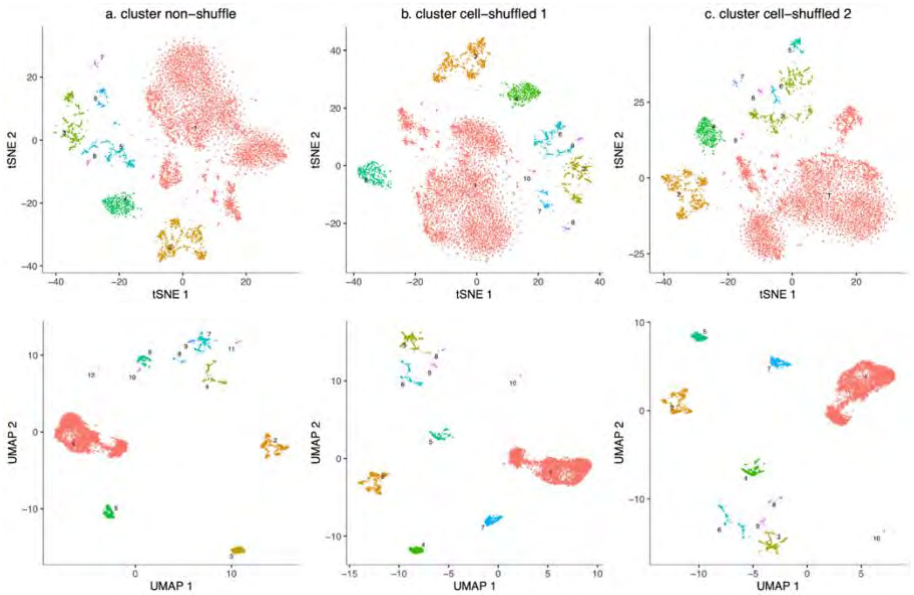

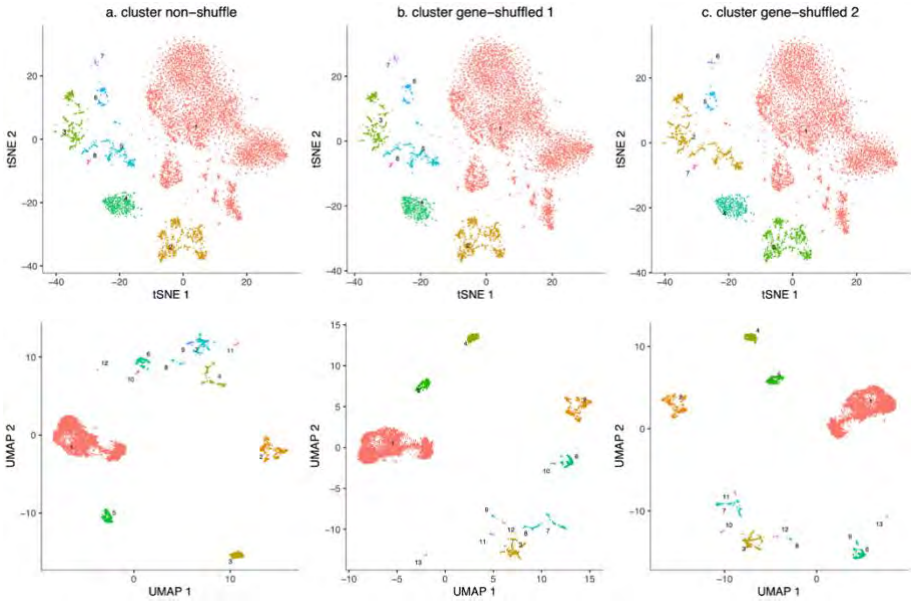

Fig. 4. Visualizations of Mouse Retina by Monocle 3 are shown in sequences original (column a), cell/gene-shuffled once (column b) and twice (column c) for t-SNE (the first and third rows) and UMAP (the second and fourth rows) with color by cell type.

Overall, while t-SNE and UMAP both retain major group separations after shuffling, the observed reorganization of biologically related clusters highlights that apparent stability in 2D layouts can mask changes in underlying neighbor relations. These findings emphasize that global position shifts, though visually subtle, can alter the biological meaning inferred from trajectory or lineage-based single-cell analyses.

3.2 Quantification

We use four quantitative methods to compare differences after shuffling: *knn*-preservation, internal evaluation indexes, Jaccard Index, and RF-hierarchical.

3.2.1 knn-preservation after dimensionality reduction

Supplemental Table 1 summarizes the *knn*-preservation rates (%) for t-SNE and UMAP from native space to each 2D plane. The rates from native space to non-shuffled data are similar to those for cell-shuffled 1 and cell-shuffled 2 across each *k* value. Table 2 summarizes the *knn*-preservation rates for the shuffled 2D plane across all datasets, showing gene shuffle keep more neighboring relation than cell shuffle.

Table 2. *knn*-preservation (%) between non-shuffle and shuffled data for different *k* value.

comparison		t-SNE				UMAP			
	k	3	10	100	1000	3	10	100	1000
C. elegans-dis									
non-shu. x cell-shu.		50.80	65.60	77.98	68.75	11.56	26.52	66.83	77.01
non-shu. x gene-shu.		73.74	84.67	92.52	93.36	11.79	27.28	67.71	78.34

C. elegans-con								
non-shu. x cell-shu.	58.21	70.66	82.12	65.79	23.16	48.90	84.79	78.05
non-shu. x gene-shu.	75.86	86.00	93.89	94.37	21.06	44.62	80.00	70.25
SCP345								
non-shu. x cell-shu.	47.90	65.45	79.26	79.68	12.55	28.66	72.88	90.41
non-shu. x gene-shu.	57.97	73.55	85.69	89.96	12.12	28.52	72.79	88.64
SCP1526								
non-shu. x cell-shu.	30.13	45.68	65.65	68.59	7.06	17.63	53.02	79.16
non-shu. x gene-shu.	51.45	68.26	84.72	90.88	7.10	17.63	53.04	79.37
Mouse Retina								
non-shu. x cell-shu.	55.02	67.45	80.75	82.61	17.00	36.86	77.89	85.04
non-shu. x gene-shu.	68.28	78.87	89.77	95.10	18.00	37.84	78.20	86.72
Mouse Brain								
non-shu. x cell-shu.	56.66	68.59	81.65	64.56	18.53	39.19	82.95	86.87
non-shu. x gene-shu.	59.04	71.30	84.49	88.37	18.42	39.57	82.71	84.90

3.2.2 Internal Evaluation

We use the CH, DB, and XB for internal evaluation, shuffling the data 100 times to obtain the mean and standard deviation. Higher CH values indicate better clustering, while lower DB and XB values are preferable. Table 3 shows these indexes for *C. elegans*-dis and *C. elegans*-con with t-SNE and UMAP. For UMAP on *C. elegans*-dis, CH and DB increase, and XB decreases in all cases, indicating better trends for CH and XB, but worse for DB. For *C. elegans*-con, all three indexes improve under all conditions.

Table 3. The three internal evaluations. The non-shuffle condition is shown by the value itself; the shuffled condition is shown as mean among 100 shuffle tests (detail standard deviation is in Supplemental Table 2). CH: Calinski-Harabasz index (log10), DB: Davies-Bouldin index, and XB: Xie-Beni index (log10) of t-SNE and UMAP.

condition	t-SNE			UMAP		
	CH↑	DB↓	XB↓	CH↑	DB↓	XB↓
C. elegans-dis						
non-shuffle-cluster	3.754	0.786	**3.022**	4.379	**0.377**	2.655
cell-shuffled-cluster	**3.894**	**0.762**	3.469	4.540	0.423	2.138
gene-shuffled-cluster	3.802	0.820	3.481	**4.544**	0.426	**2.009**
C. elegans-con						
non-shuffle-cluster	3.214	0.862	4.027	3.686	0.849	3.085
cell-shuffled-cluster	**3.244**	0.862	3.347	**3.729**	**0.636**	2.933

condition	t-SNE			UMAP		
	CH↑	DB↓	XB↓	CH↑	DB↓	XB↓
gene-shuffled-cluster	3.201	**0.775**	**3.355**	3.713	0.663	**2.819**
SCP345						
non-shuffle-cluster	**4.009**	**0.769**	3.265	4.440	**0.415**	**1.083**
cell-shuffled-cluster	3.870	0.771	**2.681**	**4.446**	0.475	1.603
gene-shuffled-cluster	3.912	0.847	2.890	4.436	0.473	1.615
SCP1526						
non-shuffle-cluster	4.350	0.799	**2.628**	5.043	0.479	**2.170**
cell-shuffled-cluster	**4.394**	**0.795**	3.056	**5.160**	0.473	2.392
gene-shuffled-cluster	4.375	0.804	2.950	5.134	**0.467**	2.282

3.2.3 Jaccard Index

Table 4 summarizes average Jaccard Index (JI) values cross data sets. UMAP results show that the lowest JI values are found in gene-shuffled conditions for *C. elegans*-dis (0.70 for both gene-shuffled 1 and 2). Supplemental Table 4 shows JI for the first ten clusters. Some clusters are highly stable (e.g., cluster 1), while others are not (e.g., cluster 5). Based on cell-shuffled 1, there are 30 stable, 4 medium stable, and 17 non-stable groups. Overall, UMAP results indicate cell-shuffling is more stable than gene-shuffling, whereas the opposite is true for t-SNE (Supplemental Table 3).

For *C. elegans*-con clustering, the t-SNE result under cell-shuffled 1 is less stable (JI < 0.6). UMAP results are highly stable in the cell-shuffled condition (JI > 0.85), but less stable in the gene-shuffled condition (JI ~ 0.75).

In the SCP345 t-SNE results, some JI values are moderately stable (~0.75). In the UMAP results, the number of clusters remains six, with JI values close to 1, indicating high stability even after shuffling. In SCP1526, t-SNE is very stable for gene-shuffled 2, while other sets are moderately stable. In UMAP result, the cell-shuffled condition is very stable (>0.85), but gene-shuffled 2 is less stable (<0.75).

For the Mouse Retina dataset, the cluster of t-SNE and UMAP are moderate stability across all conditions. For the Mouse Brain dataset, the JI value is close to 1 for all UMAP conditions and gene-shuffled t-SNE, indicating some datasets are unaffected by shuffling.

Table 4. The average JI of all data sets and its detail supplemental tables shown in brackets.

comparison	t-SNE	UMAP
C. elegans-dis (Supplemental Tables 3 and 4)		
non-shuffle vs cell-shuffled 1	0.74	0.72
non-shuffle vs cell-shuffled 2	0.85	**0.84**

non-shuffle vs gene-shuffled 1	**0.95**	0.70
non-shuffle vs gene-shuffled 2	0.88	0.70
C. elegans-con (Supplemental Tables 5 and 6)		
non-shuffle vs cell-shuffled 1	0.59	**0.92**
non-shuffle vs cell-shuffled 2	0.72	0.88
non-shuffle vs gene-shuffled 1	**0.83**	0.74
non-shuffle vs gene-shuffled 2	0.66	0.76
SCP345 (Supplemental Tables 7 and 8)		
non-shuffle vs cell-shuffled 1	**0.96**	0.98
non-shuffle vs cell-shuffled 2	0.74	0.98
non-shuffle vs gene-shuffled 1	0.96	**0.99**
non-shuffle vs gene-shuffled 2	0.73	0.98
SCP1526 (Supplemental Tables 9 and 10)		
non-shuffle vs cell-shuffled 1	0.72	0.85
non-shuffle vs cell-shuffled 2	0.73	**0.86**
non-shuffle vs gene-shuffled 1	0.76	0.85
non-shuffle vs gene-shuffled 2	**0.90**	0.68
Mouse Retina (Supplemental Tables 11 and 12)		
non-shuffle vs cell-shuffled 1	0.98	0.78
non-shuffle vs cell-shuffled 2	0.73	0.82
non-shuffle vs gene-shuffled 1	**1.00**	0.85
non-shuffle vs gene-shuffled 2	0.87	**0.87**
Mouse Brain (Supplemental Tables 13 and 14)		
non-shuffle vs cell-shuffled 1	0.74	0.97
non-shuffle vs cell-shuffled 2	0.68	**0.98**
non-shuffle vs gene-shuffled 1	**1.00**	0.96
non-shuffle vs gene-shuffled 2	**1.00**	0.96

3.2.4 RF-hierarchical

Table 5 shows the Robinson-Foulds (RF) Distance between non-shuffled and shuffled sets. For UMAP, *C. elegans*-dis has an RF of 52 (out of 54), and *C. elegans*-con has an RF of 48, indicating unstable global structures. The SCP345 dataset, with a worst-case RF of 10, has an RF of 2, showing some global structure preservation. SCP1526, with a worst-case RF of 16, also shows significant changes post-shuffling. In contrast, t-SNE RF values are generally lower, and PCA RF values are all 0, indicating stable global structures.

Table 5. The Robinson-Foulds distance comparison with each set where the maximum RF-hierarchical of the set is shown in the row of the dataset. The ratio compared with the maximum RF is shown in proportion, and the maximum RF is labelled beside the name of the dataset.

comparison	t-SNE	UMAP
C. elegans-dis, 54		
non-shuffle vs cell-shuffled 1	46 (85%)	52 (96%)
non-shuffle vs cell-shuffled 2	46 (85%)	52 (96%)
non-shuffle vs gene-shuffled 1	**4** (7%)	52 (96%)
non-shuffle vs gene-shuffled 2	18 (33%)	52 (96%)
C. elegans-con, 48		
non-shuffle vs cell-shuffled 1	34 (71%)	**22** (46%)
non-shuffle vs cell-shuffled 2	30 (63%)	26 (54%)
non-shuffle vs gene-shuffled 1	**20** (42%)	34 (71%)
non-shuffle vs gene-shuffled 2	24 (50%)	**22** (46%)
SCP345, 10		
non-shuffle vs cell-shuffled 1	2 (20%)	4 (40%)
non-shuffle vs cell-shuffled 2	8 (80%)	4 (40%)
non-shuffle vs gene-shuffled 1	**0** (0%)	4 (40%)
non-shuffle vs gene-shuffled 2	8 (80%)	4 (40%)
SCP1526, 16		
non-shuffle vs cell-shuffled 1	14 (88%)	16 (100%)
non-shuffle vs cell-shuffled 2	14 (88%)	16 (100%)
non-shuffle vs gene-shuffled 1	8 (50%)	16 (100%)
non-shuffle vs gene-shuffled 2	**6** (38%)	16 (100%)

Supplemental Figures 7 to 22 show UPGMA clustering results. Supplemental Figures 8a to 8c correspond to Figures 2a the second row (*C. elegans*-dis). Initially, Coelomocytes are nearest to Rectum, Non-seam hypodermis, and Seam cells. After the first shuffle, Coelomocytes are closer to Failed QC. In the second shuffle, Coelomocytes are distant from all other types in both Supplemental Figures 8c and Figures 2a the second row – column c.

Quantitative evaluations show that t-SNE and UMAP retain similar *knn*-preservation levels before and after shuffling, indicating limited changes in local neighbor relations. UMAP generally performs better in internal clustering metrics, with CH scores rising after shuffling, although DB and XB often show mixed trends. However, clustering consistency is not always maintained: t-SNE on *C. elegans-con* under cell-shuffling (JI = 0.59) and UMAP on SCP1526 under gene-shuffling (JI ≈ 0.70) both reveal notable instability. Global structure is even more affected: UMAP reaches the worst RF-hierarchical value for SCP1526, and t-SNE approaches it, particularly in larger datasets. In contrast, PCA consistently yields RF = 0, indicating stable global relationships.

Overall, while t-SNE and UMAP preserve some local structure, their internal evaluation scores, Jaccard stability, and RF-hierarchical results show substantial sensitivity to input shuffling. These findings demonstrate that nonlinear dimensionality reduction methods cannot be assumed stable without explicitly accounting for variations in input ordering.

4 Conclusion

t-SNE and UMAP are effective for visualizing high-dimensional datasets and are particularly suitable for single-cell data, often producing clear and well-separated clusters. However, our analyses demonstrate that their global structures are not stable. Although PCA remains completely stable under data shuffling, it is less effective at capturing nonlinear biological relationships and therefore cannot replace nonlinear methods in most practical scRNA-seq applications.

The instability we observed, as reflected through internal evaluation metrics, RF-hierarchical distances, and Jaccard Index analyses, shows that nonlinear dimensionality reduction techniques should not be assumed stable without accounting for variations in input ordering. Our shuffling-based evaluation highlights an additional and previously underappreciated source of nondeterminism. In contrast to earlier reports emphasizing sensitivity to initialization or random seeds [17, 18], we verified that embeddings generated with identical seeds remain consistent. The differences in our study therefore arise specifically from input-order perturbations, indicating that both initialization randomness and input ordering can meaningfully influence the reproducibility of single-cell visualizations.

These findings also suggest practical considerations for improving the reliability of scRNA-seq visualization. One useful direction is to treat shuffling not merely as a diagnostic tool but as a means of constructing consensus representations by aggregating results across multiple shuffled embeddings. Such an approach can help reveal structures that remain stable across perturbations while identifying regions of the embedding that may be unreliable. Another promising avenue involves borrowing ideas from bootstrap methodology to introduce explicit confidence measures into visualization platforms. Embedding confidence scores or uncertainty contours would allow researchers to directly assess the reliability of both local neighborhoods and global arrangements, thereby improving interpretability.

By integrating these perspectives, this work encourages a shift in how dimensionality reduction is used in single-cell analysis. Instead of relying on a single embedding as a definitive representation, researchers may benefit from incorporating stability assessments into routine workflows. Doing so would enhance the reproducibility, transparency, and biological credibility of scRNA-seq visualizations.

Acknowledgments

We would like to acknowledge the National Center for High-performance Computing (NCHC) for providing computational and storage resources. This work was supported by the National Science and Technology Council [114-2221-E-004-008]

References

[1] L. McInnes, J. Healy, and J. Melville, "UMAP: Uniform Manifold Approximation and Projection for Dimensionality reduction," *arXiv*, 2018, doi: 10.48550/arxiv.1802.03426.

[2] C. Trapnell *et al.*, "The dynamics and regulators of cell fate decisions are revealed by pseudotemporal ordering of single cells," *Nat. Biotechnol.*, vol. 32, no. 4, pp. 381–386, 2014, doi: 10.1038/nbt.2859.

[3] M. Tang *et al.*, "Evaluating single-cell cluster stability using the Jaccard similarity index," *Bioinformatics*, vol. 37, no. 15, pp. 2212–2214, 2020, doi: 10.1093/bioinformatics/btaa956.

[4] C. N. Heiser and K. S. Lau, "A Quantitative Framework for Evaluating Single-Cell Data Structure Preservation by Dimensionality Reduction Techniques," *Cell Rep.*, vol. 31, no. 5, p. 107576, 2020, doi: 10.1016/j.celrep.2020.107576.

[5] X. Liu *et al.*, "A comparison framework and guideline of clustering methods for mass cytometry data," *Genome Biol*, vol. 20, no. 1, p. 297, 2019, doi: 10.1186/s13059-019-1917-7.

[6] M. Chatzou, E. W., P. Di, Gascuel, and Notredame, "Generalized Bootstrap Supports for Phylogenetic Analyses of Protein Sequences Incorporating Alignment Uncertainty," *Systematic Biology*, 2018, doi: 10.1093/sysbio/syx096.

[7] J. Cao *et al.*, "Comprehensive single-cell transcriptional profiling of a multicellular organism," *Science*, vol. 357, no. 6352, pp. 661–667, 2017, doi: 10.1126/science.aam8940.

[8] J. S. Packer *et al.*, "A lineage-resolved molecular atlas of C. elegans embryogenesis at single-cell resolution," *Science*, vol. 365, no. 6459, 2019, doi: 10.1126/science.aax1971.

[9] D. Balboa *et al.*, "Functional, metabolic and transcriptional maturation of human pancreatic islets derived from stem cells," *Nat. Biotechnol.*, vol. 40, no. 7, pp. 1042–1055, 2022, doi: 10.1038/s41587-022-01219-z.

[10] E. Z. Macosko *et al.*, "Highly Parallel Genome-wide Expression Profiling of Individual Cells Using Nanoliter Droplets," *Cell*, vol. 161, no. 5, pp. 1202–1214, 2015, doi: 10.1016/j.cell.2015.05.002.

[11] M. Ximerakis *et al.*, "Single-cell transcriptomic profiling of the aging mouse brain," *Nat. Neurosci.*, vol. 22, no. 10, pp. 1696–1708, 2019, doi: 10.1038/s41593-019-0491-3.

[12] D. F. Robinson and L. R. Foulds, “Comparison of phylogenetic trees,” *Math. Biosci.*, vol. 53, no. 1–2, pp. 131–147, 1981, doi: 10.1016/0025-5564(81)90043-2.

[13] C. D. Michener and R. R. Sokal, “A QUANTITATIVE APPROACH TO A PROBLEM IN CLASSIFICATION†,” *Evol. Int. J. Org. Evol.*, vol. 11, no. 2, pp. 130–162, 1957, doi: 10.1111/j.1558-5646.1957.tb02884.x.

[14] T. Caliński and J. Harabasz, “A dendrite method for cluster analysis,” *Commun. Stat.*, vol. 3, no. 1, pp. 1–27, 1974, doi: 10.1080/03610927408827101.

[15] D. L. Davies and D. W. Bouldin, “A cluster separation measure.,” *IEEE Trans. pattern Anal. Mach. Intell.*, vol. 1, no. 2, pp. 224–7, 1979.

[16] X. L. Xie and G. Beni, “A validity measure for fuzzy clustering,” *IEEE Trans. Pattern Anal. Mach. Intell.*, vol. 13, no. 8, pp. 841–847, 2024, doi: 10.1109/34.85677.

[17] W. Kobak and P. Berens, “The art of using t-SNE for single-cell transcriptomics,” *Nat. Commun.*, vol. 10, no. 1, p. 5416, 2019.

[18] B. Becht et al., “Dimensionality reduction for visualizing single-cell data using UMAP,” *Nat. Biotechnol*., vol. 39, no. 12, pp. 1480–1490, 2021.

Stability of Single-Cell Dimensionality Reduction Following Shuffling Test

1. Calinski-Harabasz index

The *Calinski-Harabasz* (CH) index applies two statistical indicators, Between-Group Sum of Squares (*BGSS*) and the Within-Group Sum of Squares (*WGSS*). *BGSS* measures the difference between each cluster's centroid (whole variance):

$$BGSS = \sum_{k=1}^{K} N_k \|G_k - G\|^2$$

, where K is the number of the clusters, N is the number of the data points, N_k is the number of points in the k^{th} cluster, G_k denotes the centroid for k^{th} cluster and G is the centroid of whole points. $||G_k - G||^2$ is the sum of the squared distances between the k^{th} cluster's centroid and the entire points' centroid. $||M_{ik} - M_{jk}||^2$ is the sum of the squared distances between i and j points in the k^{th} cluster. *WGSS* represents the differences within each cluster (local variance):

$$WGSS = \sum_{k=1}^{K} \frac{1}{N_k} \sum_{i<j \in N_k} \left\| M_{ik} - M_{jk} \right\|^2$$

, M_{ik} and M_{jk} denote the observations of point i and j in the kth cluster. $||M_{ik} - M_{jk}||^2$ is the sum of the squared distances between i and j points in the k^{th} cluster. So, a clustering should have the larger BGSS and the smaller WGSS. That is, the higher the CH score is, the better a clustering based on the following equation:

$$CH = \frac{BGSS/(K-1)}{WGSS/(N-K)} = \frac{BGSS * (N-K)}{WGSS * (K-1)}$$

2. Davies-Bouldin index

The *Davies-Bouldin* (DB) index is the average similarity between each cluster, a lower DB index is associated with a model with better separation between clusters. First, we calculate the similarity defined as $R_{kk'}$:

$$R_{kk'} = \frac{S_k + S_{k'}}{d_{kk'}}$$

, where S_k and $S_{k'}$ are the average distance between each point of cluster k / k' and the centroid of that cluster. $d_{kk'}$ denotes the distance between the cluster centroid of k and k':

$$d_{kk'} = \|G_k - G_{k'}\|$$

The final DB formula is:

$$DB = \frac{1}{K} \sum_{k=1}^{K} \max R_{kk'}, k \neq k'$$

3. Xie-Beni Index

Xie-Beni (XB) index also uses the WGSS statistical indicator, which is used to be divided by the minimum of the least squared distance between points in the cluster:

$$D(k, k') = \min d(M_{ik}, M_{jk'})$$

That is, the XB formula can be written as:

$$XB = \frac{1}{N}\frac{WGSS}{\min D(k,k')^2}, k < k'$$

, where *N* is the total number of points. *k* and *k*' are the cluster labels, and *k* is always smaller than *k*'. By the formula of XB, the smaller the WGSS is, the smaller the XB is, and the better clustering is.

4. Jaccard Index

The index is calculated using the formula:

$$JI(A,B) = \frac{|A \cap B|}{|A \cup B|}$$

, where *A* represents an original cluster and *B* represents a cluster after shuffling. $|A \cap B|$ represents the intersection of the same cluster labels between *A* and *B* (i.e., how many cells are in common between *A* and *B*). $|A \cup B|$ is the union of *A* and *B*.

Supplemental Figures

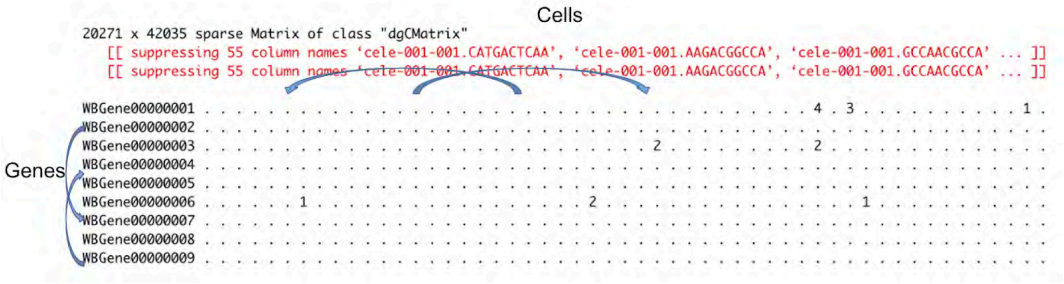

Supplemental Figure 1. Shuffle the sparse matrix (blue arrow) by row (gene) or column (cell).

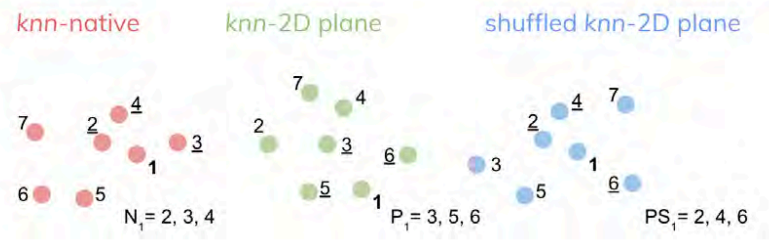

Supplemental Figure 2. An example of *knn*-preservation where *k*=3. The pink, green and blue points represent cells in the *knn*-native, *knn*-2D, and *knn*-2D planes. The target cell, 1, is marked as bold and its neighbors as underlined.

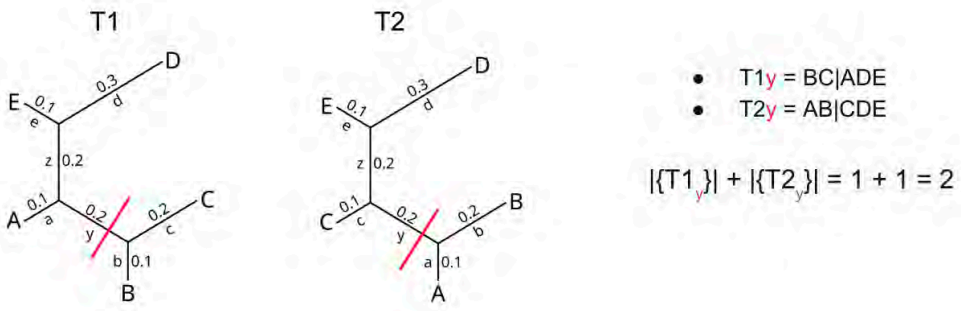

Supplemental Figure 3. An example of RF distance. T1 and T2 have five leaves and two internal branches *z* and *y*. When cutting the branch z, T1 and T2 will be divided into two sub-trees ED|ABC. When cutting to y, T1 will be divided into BC|ADE, and T2 will be cut into AB|CDE, so the RF value in this sample is 1 + 1 = 2.

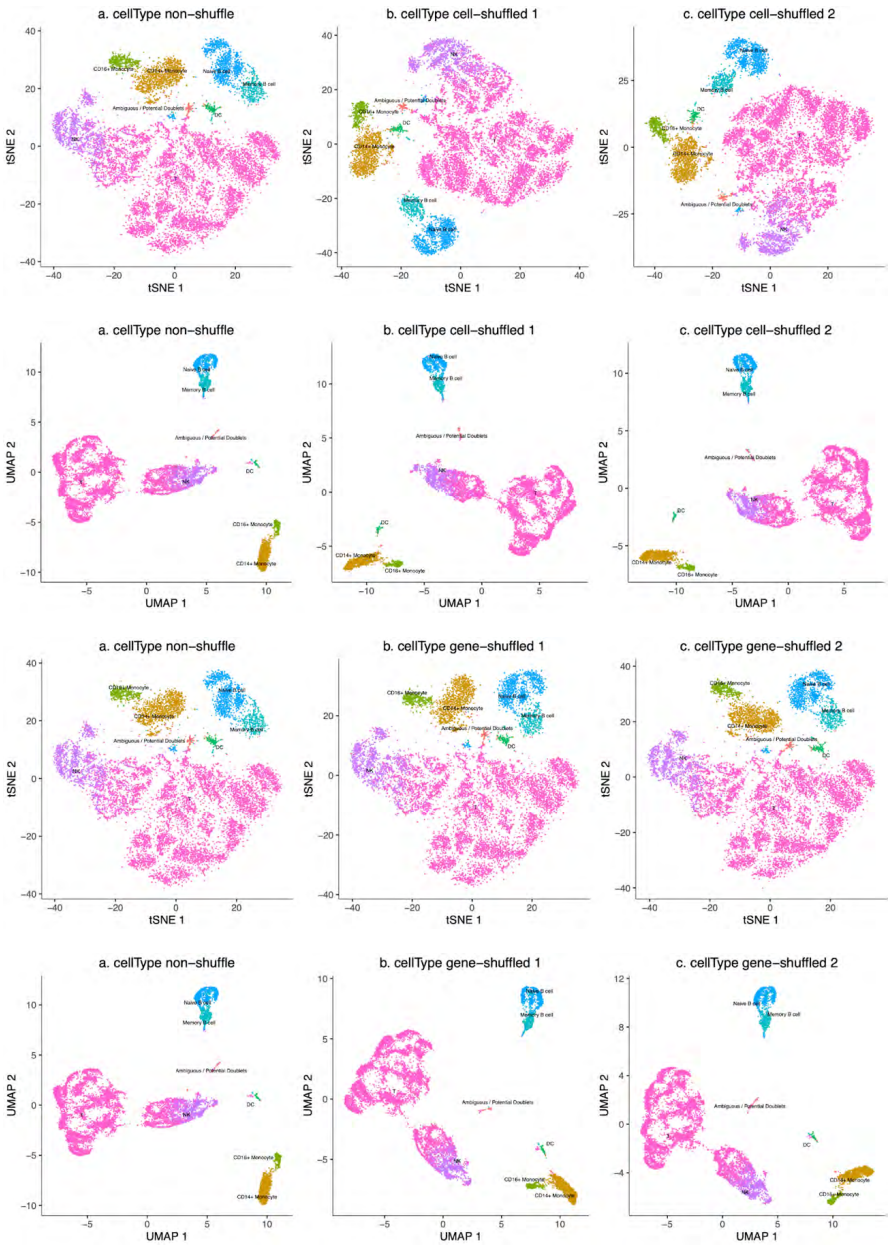

Supplemental Figure 4. Visualizations of SCP345 by Monocle 3 are shown in sequences: original (column a), cell/gene-shuffled once (column b) and twice (column c) for t-SNE (the first and third rows) and UMAP (the second and fourth rows) with color by cell type.

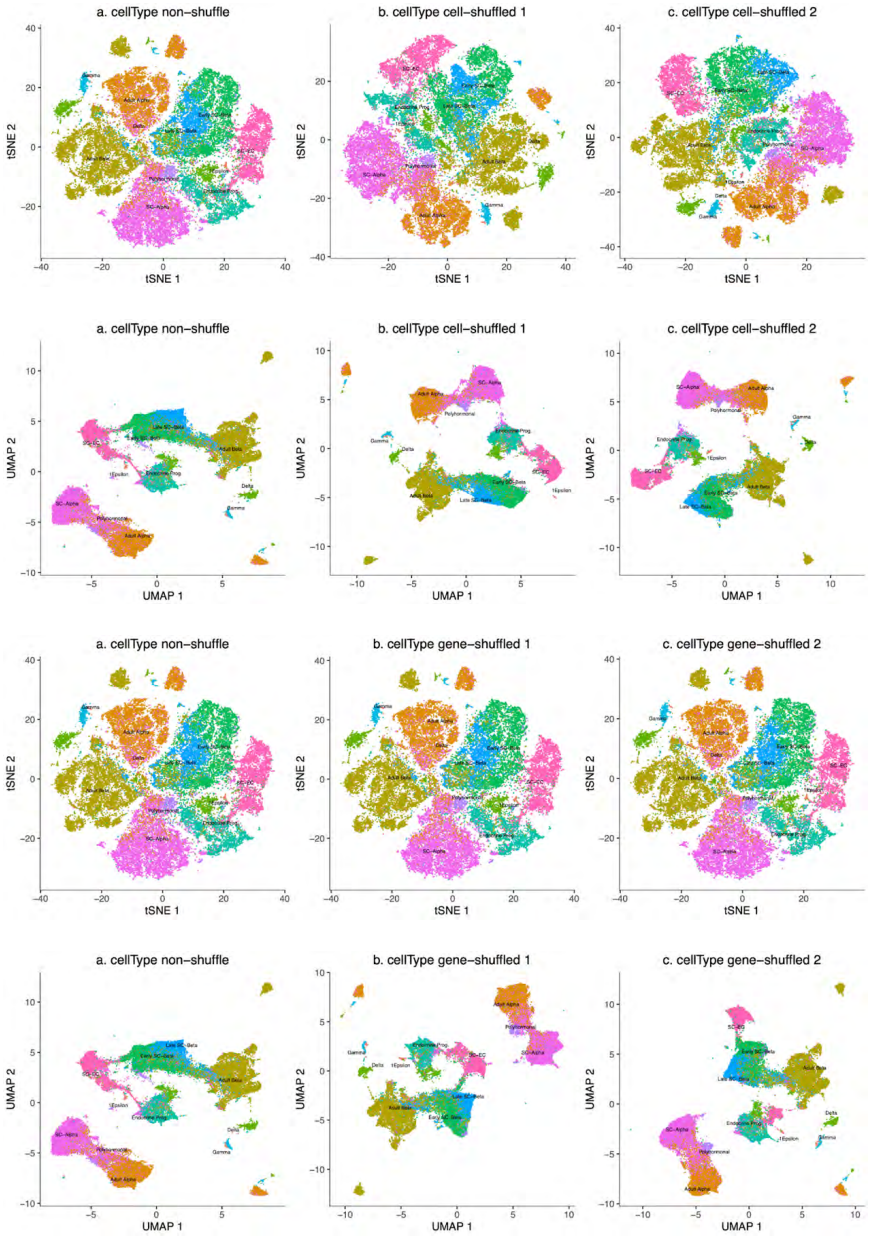

Supplemental Figure 5. Visualizations of SCP1526 by Monocle 3 are shown in sequences: original (column a), cell/gene-shuffled once (column b) and twice (column c) for t-SNE (the first and third rows) and UMAP (the second and fourth rows) with color by cell type.

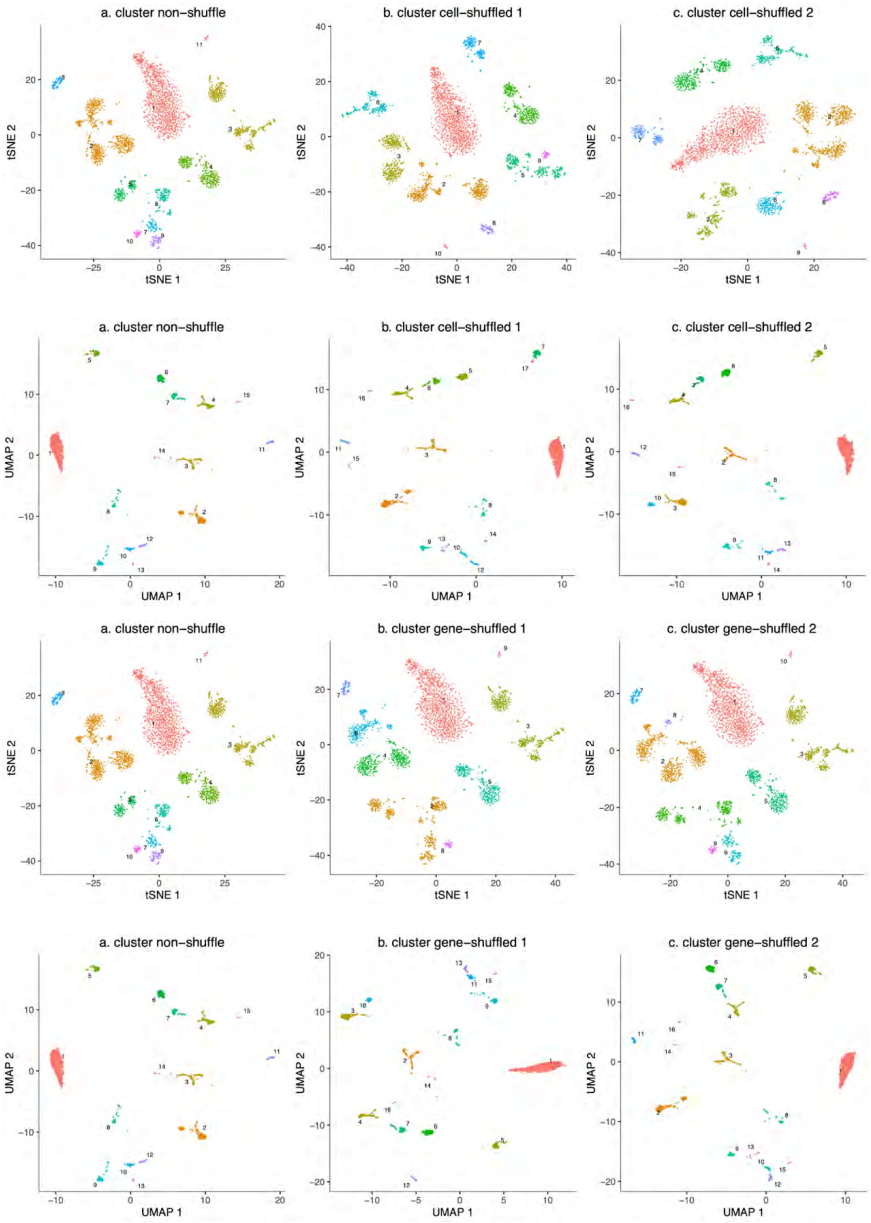

Supplemental Figure 6. Visualizations of Mouse Brain by Monocle 3 are shown in sequences: original (a, d, g), gene-shuffled once (b, e, h), and gene-shuffled twice (c, f, i). These are labeled by Cao cell type (a-c), cluster result (d-f), and partition (g-i), with Coelomocytes highlighted in a red circle.

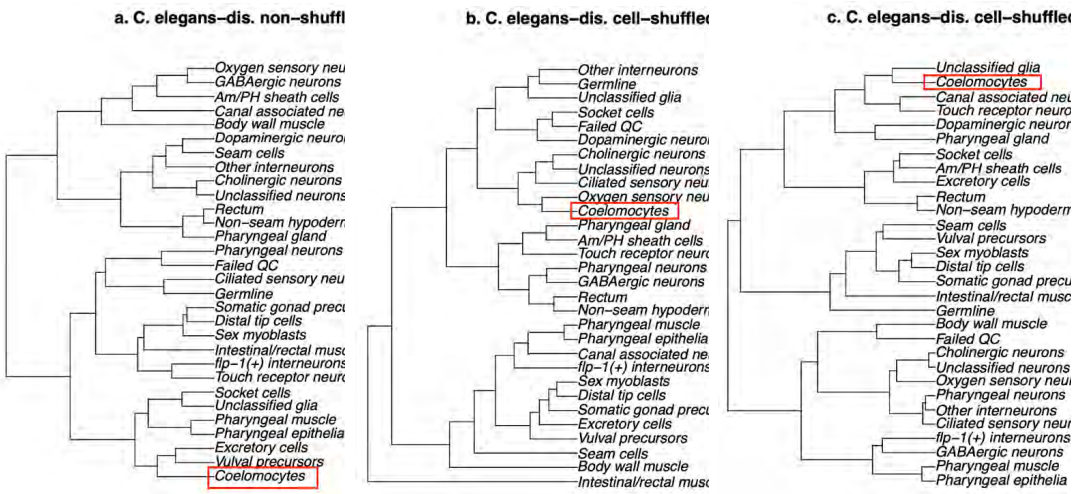

Supplemental Figure 7. UPGMA results of t-SNE, non-shuffle (a), cell-shuffled 1 (b), and cell-shuffled 2 (c) with the label of Cao cell type for *C. elegans*-dis. The Coelomocytes cell is marked as a red rectangle.

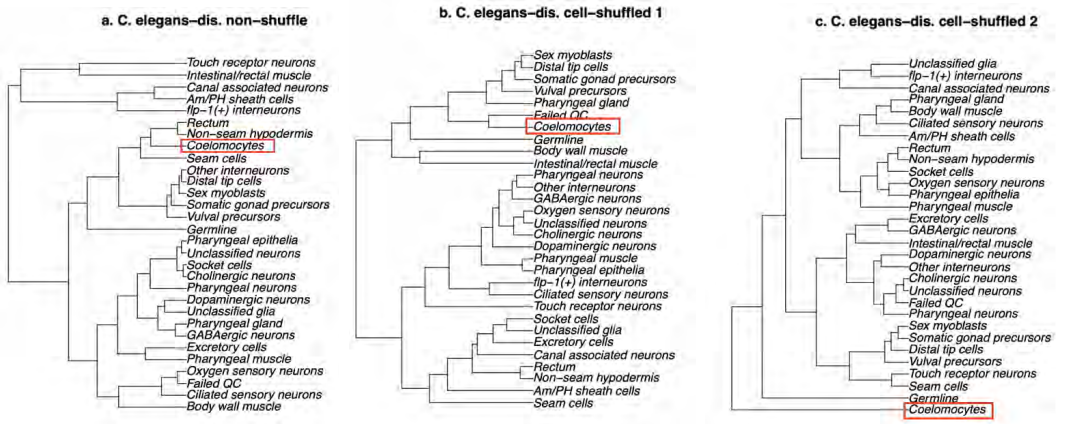

Supplemental Figure 8. UPGMA results of UMAP, non-shuffle (a), cell-shuffled 1 (b), and cell-shuffled 2 (c) with the label of Cao cell type for *C. elegans*-dis. The Coelomocytes cell is marked as a red rectangle.

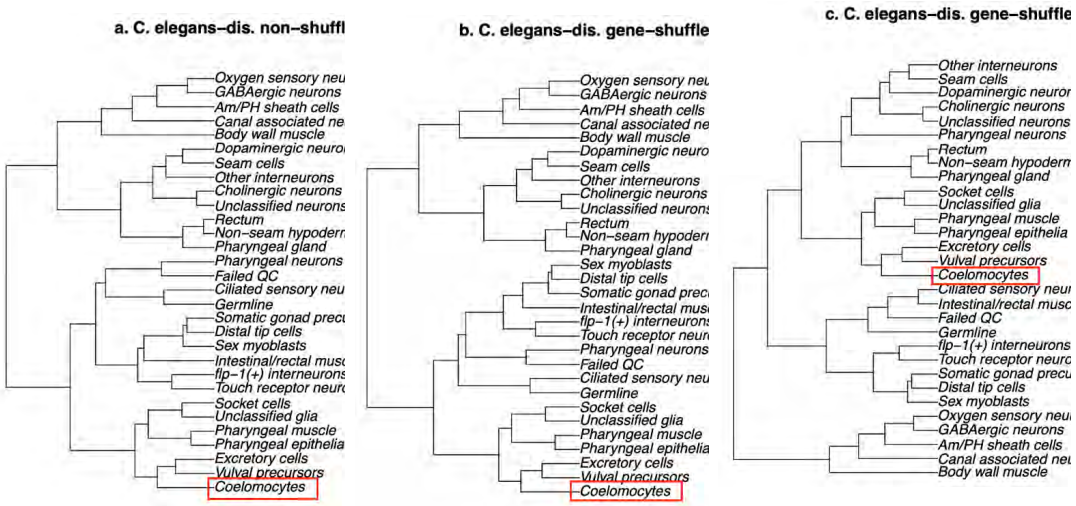

Supplemental Figure 9. UPGMA results of t-SNE, non-shuffle (a), gene-shuffled 1 (b), and gene-shuffled 2 (c) with the label of Cao cell type for *C. elegans*-dis. The Coelomocytes cell is marked as a red rectangle.

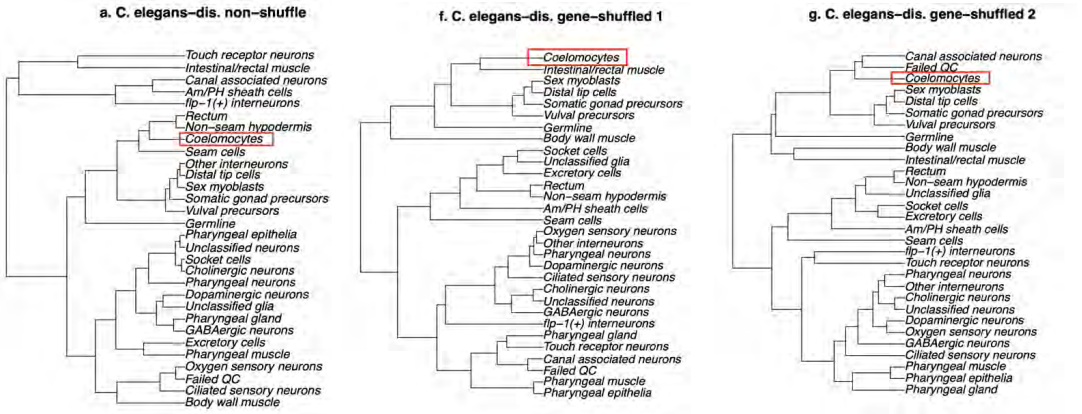

Supplemental Figure 10. UPGMA results of UMAP, non-shuffle (a), gene-shuffled 1 (b), and gene-shuffled 2 (c) with the label of Cao cell type for *C. elegans*-dis. The Coelomocytes cell is marked as a red rectangle.

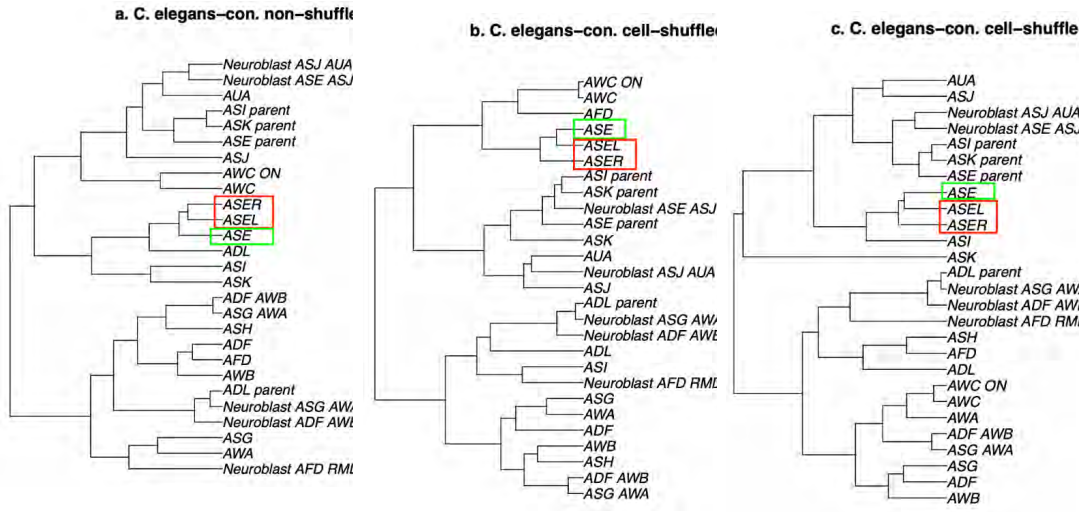

Supplemental Figure 11. UPGMA results of t-SNE, non-shuffle (a), cell-shuffled 1 (b), and cell-shuffled 2 (c) with the label of Cao cell type for *C. elegans*-con. ASE is the parent of ASER and ASEL marked with a green rectangle. ASER and ASEL are marked as red rectangles.

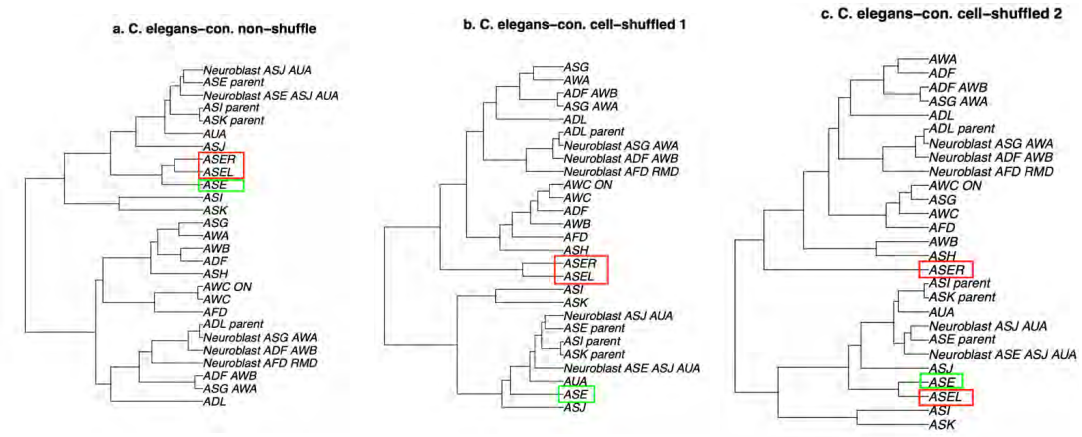

Supplemental Figure 12. UPGMA results of UMAP, non-shuffle (a), cell-shuffled 1 (b), and cell-shuffled 2 (c) with the label of Cao cell type for *C. elegans*-con. ASE is the parent of ASER and ASEL marked with a green rectangle. ASER and ASEL are marked as red rectangles.

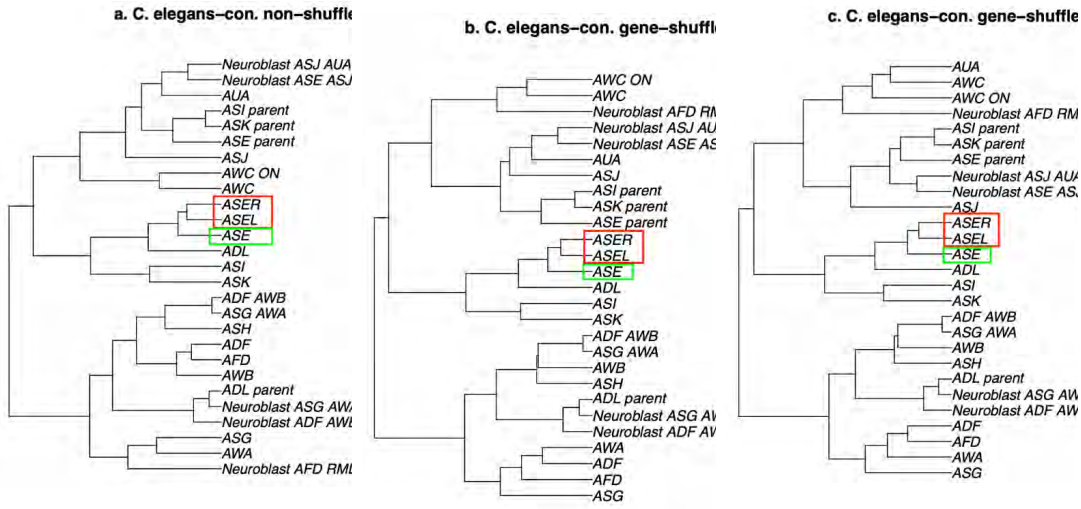

Supplemental Figure 13. UPGMA results of t-SNE non-shuffle (a), gene-shuffled 1 (b), and gene-shuffled 2 (c) with the label of Cao cell type for *C. elegans*-con. ASE is the parent of ASER and ASEL marked with a green rectangle. ASER and ASEL are marked as red rectangles.

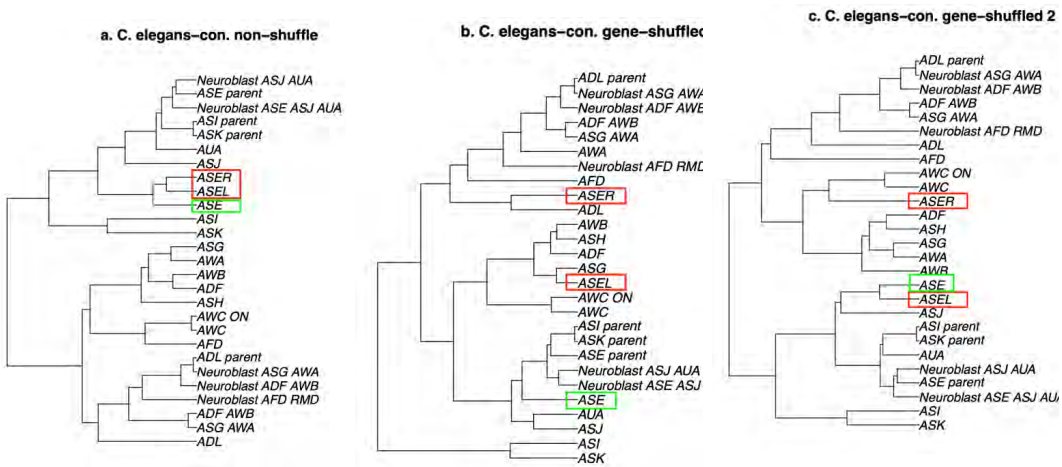

Supplemental Figure 14. UPGMA results of UMAP, non-shuffle (a), gene-shuffled 1 (b), and gene-shuffled 2 (c) with the label of Cao cell type for *C. elegans*-con. ASE is the parent of ASER and ASEL marked with a green rectangle. ASER and ASEL are marked as red rectangles.

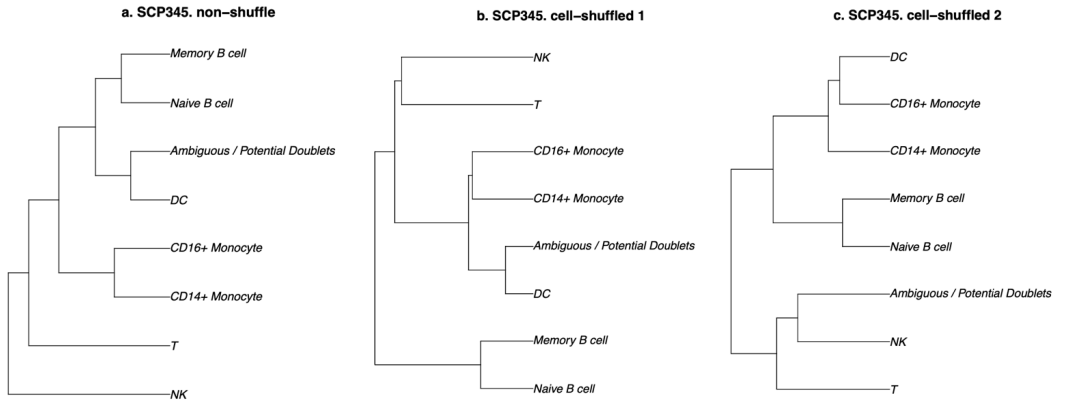

Supplemental Figure 15. UPGMA results of t-SNE non-shuffle (a), cell-shuffled 1 (b), and cell-shuffled 2 (c) with the label of cell type for SCP345.

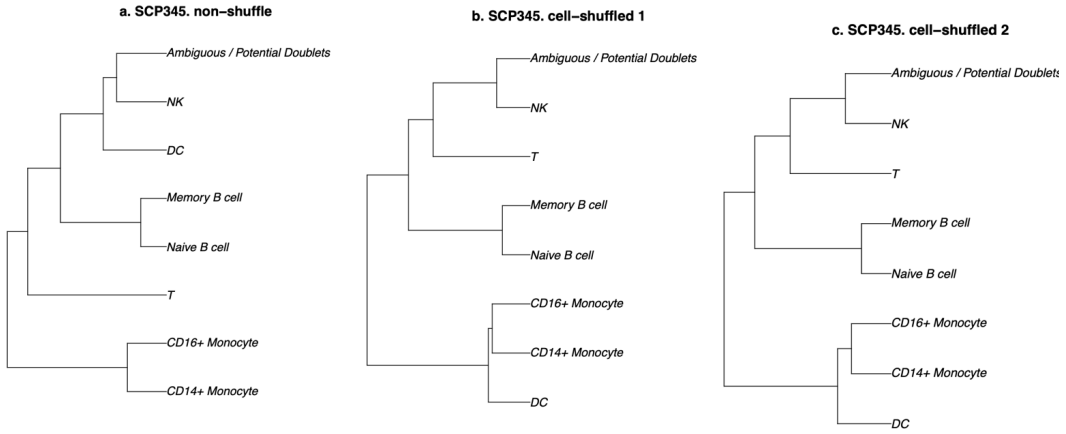

Supplemental Figure 16. UPGMA results of UMAP, non-shuffle (a), cell-shuffled 1 (b), and cell-shuffled 2 (c) with the label of cell type for SCP345.

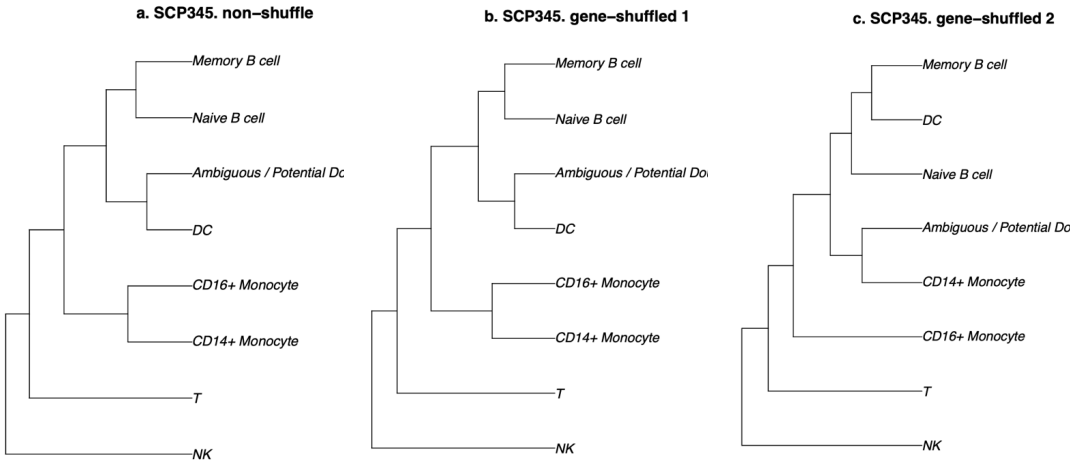

Supplemental Figure 17. UPGMA results of t-SNE, non-shuffle (a), gene-shuffled 1 (b), and gene-shuffled 2 (c) with the label of cell type for SCP345.

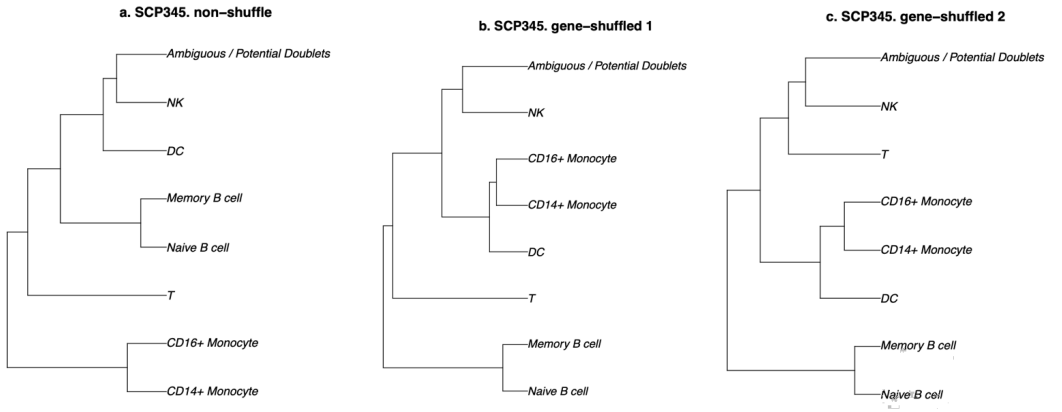

Supplemental Figure 18.UPGMA results of UMAP, non-shuffle (a), gene-shuffled 1 (b), and gene-shuffled 2 (c) with the label of cell type for SCP345.

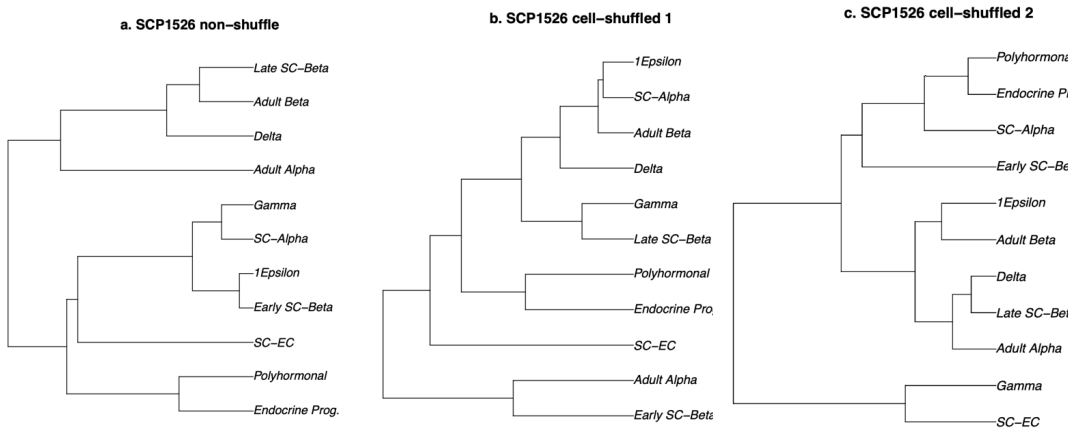

Supplemental Figure 19. UPGMA results of t-SNE non-shuffle (a), cell-shuffled 1 (b), and cell-shuffled 2 (c) with the label of cell type for SCP1526.

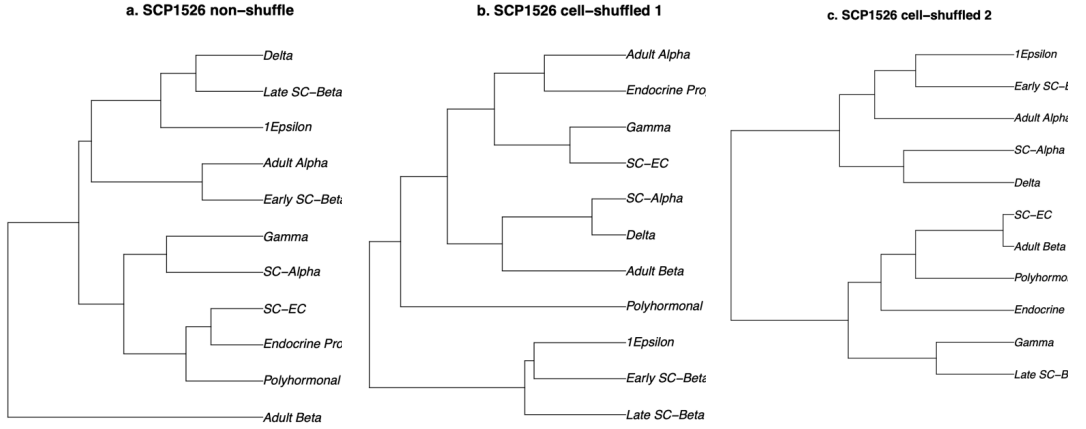

Supplemental Figure 20. UPGMA results of UMAP, non-shuffle (a), cell-shuffled 1 (b), and cell-shuffled 2 (c) with the label of cell type for SCP1526.

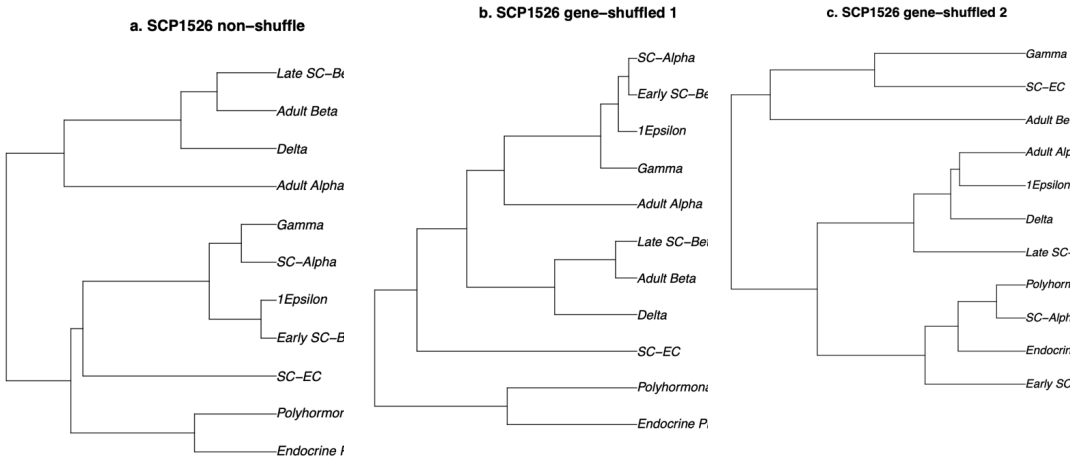

Supplemental Figure 21. UPGMA results of t-SNE non-shuffle (a), gene-shuffled 1 (b), and gene-shuffled 2 (c) with the label of cell type for SCP1526.

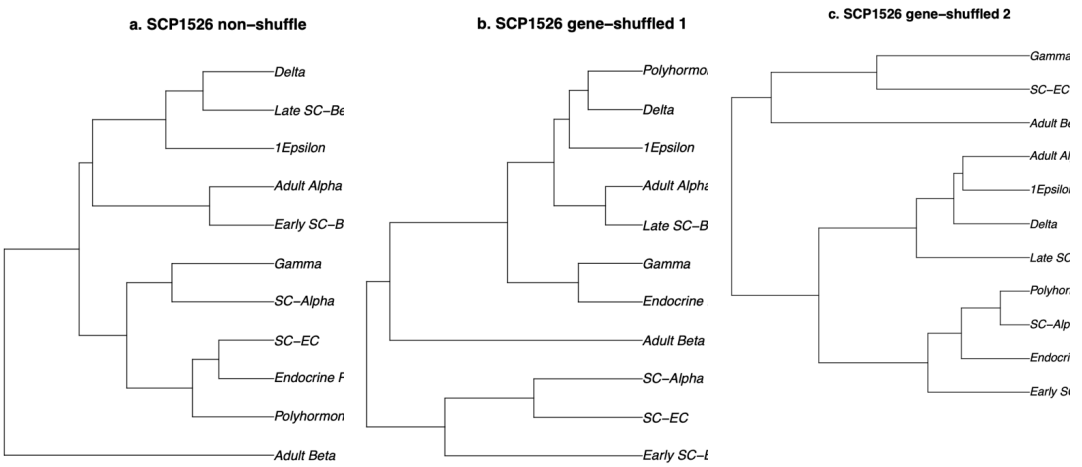

Supplemental Figure 22. UPGMA results of UMAP, non-shuffle (a), gene-shuffled 1 (b), and gene-shuffled 2 (c) with the label of cell type for SCP1526.

Supplemental Tables

Supplemental Table 1. *knn*-preservation (%) between native space and non-shuffle, for different *k* value.

comparison		t-SNE				UMAP			
	k	3	10	100	1000	3	10	100	1000
C. elegans-dis									
	nat. x non-shu.	25.60	41.84	67.58	93.91	24.40	40.68	67.67	93.35
	ave nat. x shu.	25.90	42.06	67.88	93.91	23.98	40.67	67.67	93.33
C. elegans-con									
	nat.x non-shu.	3.96	9.77	31.63	54.60	2.89	8.27	31.15	57.46
	ave nat.x shu.	3.98	9.81	31.91	54.46	2.89	8.29	31.21	54.94
SCP345									
	nat. x non-shu	2.75	7.73	31.43	81.18	3.08	7.47	31.44	83.88
	ave nat. x shu	3.16	7.71	31.65	83.10	3.15	7.46	31.74	84.15
SCP1526									
	nat. x non-shu	2.65	5.61	16.79	34.96	2.07	4.84	17.17	38.38
	ave nat. x shu	2.55	5.57	16.80	35.68	2.27	4.99	17.32	38.21
Mouse Retina									
	nat. x non-shu	4.92	22.02	76.35	97.95	4.29	22.19	75.31	98.00
	ave nat. x shu	4.93	22.29	76.30	97.82	4.29	22.04	75.30	97.95
Mouse Brain									
	nat. x non-shu	6.07	11.92	34.43	67.71	4.92	10.72	33.74	68.89
	ave nat. x shu	6.08	11.89	34.45	63.35	4.73	10.62	33.85	67.70

Supplemental Table 2. The three internal evaluations. The non-shuffle condition is shown by the value itself, the shuffled condition is shown as mean ± standard deviation among 100 shuffle tests. CH: Calinski-Harabasz index (log10), DB: Davies-Bouldin index, and XB: Xie-Beni index (log10) of t-SNE and UMAP.

condition	t-SNE			UMAP		
	CH	DB	XB	CH	DB	XB
C. elegans-dis						
non-shuffle-cluster	3.7542	0.7858	3.0222	4.3788	0.3768	2.6548
cell-shuffled-cluster	3.8941 ± 0.0819	0.7619 ± 0.0566	3.4693 ± 0.6238	4.5402 ± 0.0617	0.4232 ± 0.0408	2.1382 ± 0.5339
gene-shuffled-cluster	3.8016 ± 0.0801	0.8195 ± 0.0592	3.4813 ± 0.5810	4.5436 ± 0.0715	0.4258 ± 0.0382	2.0092 ± 0.4405
C. elegans-con						
non-shuffle-cluster	3.2137	0.8615	4.0270	3.6859	0.8485	3.0851
cell-shuffled-cluster	3.2442 ± 0.0989	0.8615 ± 0.0961	3.3471 ± 0.6229	3.7292 ± 0.0844	0.6358 ± 0.0822	2.9334 ± 0.5123
gene-shuffled-cluster	3.2008 ± 0.0728	0.7751 ± 0.0519	3.3551 ± 0.6399	3.7128 ± 0.0858	0.6627 ± 0.0902	2.8190 ± 0.3973
SCP345						
non-shuffle-cluster	4.0092	0.7691	3.2648	4.4397	0.4149	1.0831
cell-shuffled-cluster	3.8695 ± 0.2113	0.7708 ± 0.0524	2.6811 ± 0.9016	4.4457 ± 0.0773	0.4754 ± 0.0521	1.6028 ± 0.8707
gene-shuffled-cluster	3.9108 ± 0.1695	0.8473 ± 0.1053	2.8895 ± 0.6557	4.4358 ± 0.0452	0.4732 ± 0.0550	1.6150 ± 0.8172
SCP1526						
non-shuffle-cluster	4.3495	0.7988	2.6277	5.0431	0.4794	2.1698
cell-shuffled-cluster	4.3937 ± 0.0504	0.7949 ± 0.0649	3.0564 ± 0.6770	5.1600 ± 0.0513	0.4728 ± 0.0398	2.3916 ± 0.4493
gene-shuffled-cluster	4.3749 ± 0.0277	0.8042 ± 0.0312	2.9500 ± 0.4773	5.1341 ± 0.0651	0.4646 ± 0.0380	2.2815 ± 0.4270

Supplemental Table 3. JI of t-SNE between Monocle 3 (no Shuffle) and Cell/Gene-shuffled data1 (left) and data2 (right) of the *C. elegans*-dis. The number inside the brackets is the average of each cluster max JI value for each comparison.

non-shuffle_vs_cell-shuffled 1(0.72)

	1	2	3	4	5	6	7	8	9	10
1	0.99	0	0	0	0	0	0	0	0	0
2	0	0.96	0	0	0	0	0	0	0	0
3	0	0	0.9	0	0	0	0	0	0	0
4	0	0	0	0.99	0	0	0	0	0	0
5	0	0.02	0	0	0.01	0.79	0	0	0	0
6	0	0	0	0	0.97	0	0	0	0	0
7	0	0	0	0	0	0	0.76	0	0	0.15
8	0	0	0	0	0	0	0	0	1.00	0
9	0	0	0	0	0	0	0	0.78	0	0
10	0	0	0	0	0	0	0	0	0	0.43

non-shuffle_vs_cell-shuffled 2(0.84)

	1	2	3	4	5	6	7	8	9	10
1	0.99	0	0	0	0	0	0	0	0	0
2	0	0.96	0	0	0	0	0	0	0	0
3	0	0	0.95	0	0	0	0	0	0	0
4	0	0	0	0.98	0	0	0	0	0	0
5	0	0.02	0	0	0	0	0.56	0	0	0.22
6	0	0	0	0	0.97	0	0	0	0	0
7	0	0	0	0	0	0.79	0	0	0	0
8	0	0	0	0	0	0	0	1.00	0	0
9	0	0	0	0	0	0	0	0	0.47	0
10	0	0	0.03	0	0	0	0	0	0	0

non-shuffle_vs_gene-shuffled 1(0.95)

	1	2	3	4	5	6	7	8	9	10
1	0.99	0	0	0	0	0	0	0	0	0
2	0	1.00	0	0	0	0	0	0	0	0
3	0	0	0.96	0	0	0	0	0	0	0
4	0	0	0	0.92	0	0	0	0	0	0
5	0	0	0	0.04	0.55	0	0	0	0	0.07
6	0	0	0	0	0	1.00	0	0	0	0
7	0	0	0	0	0.38	0	0	0	0	0
8	0	0	0	0	0	0	1.00	0	0	0
9	0	0	0	0	0	0	0	1.00	0	0
10	0	0	0	0	0	0	0	0	1.00	0

non-shuffle_vs_gene-shuffled 2 (0.88)

	1	2	3	4	5	6	7	8	9	10
1	0.94	0	0	0	0	0	0	0	0	0
2	0	1.00	0	0	0	0	0	0	0	0
3	0.04	0	0	0.83	0	0	0	0	0	0
4	0	0	0.95	0	0	0	0	0	0	0
5	0	0	0	0	0.44	0	0	0.33	0	0
6	0	0	0	0	0	0	0	0	0.62	0
7	0	0	0	0	0.43	0	0	0	0	0
8	0	0	0	0	0	1.00	0	0	0	0
9	0	0	0	0	0	0	1.00	0	0	0
10	0	0	0	0	0	0	0	0	0	1.00

Supplemental Table 4. JI of UMAP between Monocle 3 (no Shuffle) and Cell/Gene-shuffled data1 (left) and data2 (right) of the *C. elegans*-dis. The number inside the brackets is the average of each cluster max JI value for each comparison.

non-shuffle_vs_cell-shuffled 1(0.72)

	1	2	3	4	5	6	7	8	9	10
1	0.99	0	0	0	0	0	0	0	0	0
2	0	0.96	0	0	0	0	0	0	0	0
3	0	0	0.90	0	0	0	0	0	0	0
4	0	0	0	0.99	0	0	0	0	0	0
5	0	0.02	0	0	0.01	0.79	0	0	0	0
6	0	0	0	0	0.97	0	0	0	0	0
7	0	0	0	0	0	0	0.76	0	0	0.15
8	0	0	0	0	0	0	0	0	1.00	0
9	0	0	0	0	0	0	0	0.78	0	0
10	0	0	0	0	0	0	0	0	0	0.43

non-shuffle_vs_cell-shuffled 2(0.84)

	1	2	3	4	5	6	7	8	9	10
1	0.99	0	0	0	0	0	0	0	0	0
2	0	0.96	0	0	0	0	0	0	0	0
3	0	0	0.95	0	0	0	0	0	0	0
4	0	0	0	0.98	0	0	0	0	0	0
5	0	0.02	0	0	0	0	0.56	0	0	0.22
6	0	0	0	0	0.97	0	0	0	0	0
7	0	0	0	0	0	0.79	0	0	0	0
8	0	0	0	0	0	0	0	1.00	0	0
9	0	0	0	0	0	0	0	0	0.47	0
10	0	0	0.03	0	0	0	0	0	0	0

non-shuffle_vs_gene-shuffled 1(0.70)

	1	2	3	4	5	6	7	8	9	10
1	0.99	0	0	0	0	0	0	0	0	0
2	0	0.96	0	0	0	0	0	0	0	0
3	0	0.01	0	0	0.51	0.45	0	0	0	0
4	0	0	0.91	0	0	0	0	0	0	0
5	0	0	0	0.99	0	0	0	0	0	0
6	0	0	0	0	0	0	0.69	0	0	0.15
7	0	0	0	0	0	0	0	0	1.00	0
8	0	0	0	0	0	0	0	0.79	0	0
9	0	0	0	0	0	0	0	0	0	0.44
10	0	0	0.09	0	0	0	0	0	0	0

non-shuffle_vs_gene-shuffled 2 (0.70)

	1	2	3	4	5	6	7	8	9	10
1	0.99	0	0	0	0	0	0	0	0	0
2	0	0.96	0	0	0	0	0	0	0	0
3	0	0.01	0	0	0	0.5	0.45	0	0	0
4	0	0	0.9	0	0	0	0	0	0	0
5	0	0	0	0.99	0	0	0	0	0	0
6	0	0	0	0	0.68	0	0	0	0	0
7	0	0	0	0	0	0	0	0	1.00	0
8	0	0	0	0	0	0	0	0.79	0	0
9	0	0	0	0	0.16	0	0	0	0	0
10	0	0	0.09	0	0	0	0	0	0	0

Supplemental Table 5. JI of t-SNE between Monocle 3 (no Shuffle) and Cell/Gene-shuffled data1 (left) and data2 (right) of the *C.elegans*-con. The number inside the brackets is the average JI value for each comparison.

non-shuffle_vs_cell-shuffled 1(0.59)

	1	2	3	4	5	6	7	8	9
1	0.53	0.2	0	0.01	0.02	0	0	0	0
2	0.29	0	0	0	0	0	0.16	0	0
3	0	0.23	0	0	0	0	0	0.31	0
4	0	0	0.98	0	0	0	0	0	0
5	0	0.22	0	0	0	0	0	0	0
6	0	0	0	0	0.75	0	0	0	0
7	0	0	0	0	0	0.98	0	0	0
8	0	0	0	0.56	0	0	0	0	0
9	0	0	0	0	0	0	0	0	0.97
10	0	0	0	0.32	0	0	0	0	0

non-shuffle_vs_cell-shuffled 2 (0.72)

	1	2	3	4	5	6	7	8	9	10
1	0.81	0.03	0.03	0	0	0	0	0	0	0.06
2	0	0.90	0	0	0	0	0	0	0	0
3	0.06	0	0	0	0.24	0	0	0	0.33	0
4	0	0	0	0.97	0	0	0	0	0	0
5	0	0	0.77	0	0	0	0	0	0	0
6	0	0	0	0	0	0	1.00	0	0	0
7	0	0	0	0	0	0	0	0.99	0	0
8	0	0	0	0	0	0.63	0	0	0	0
9	0	0	0	0	0.44	0	0	0	0	0
10	0	0	0	0	0	0.36	0	0	0	0

non-shuffle_vs_gene-shuffled 1 (0.83)

	1	2	3	4	5	6	7	8	9	10	11
1	0.98	0	0	0	0	0	0	0	0	0	0
2	0.02	0.51	0.44	0	0	0	0	0	0	0	0
3	0	0	0	0.85	0	0	0	0	0	0	0.15
4	0	0	0	0	1.00	0	0	0	0	0	0
5	0	0	0	0	0	1.00	0	0	0	0	0
6	0	0	0	0	0	0	0	1.00	0	0	0
7	0	0	0	0	0	0	0	0	1.00	0	0
8	0	0	0	0	0	0	0.63	0	0	0	0
9	0	0	0	0	0	0	0	0	0	1.00	0
10	0	0	0	0	0	0	0.37	0	0	0	0

non-shuffle_vs_gene-shuffled 2 (0.66)

	1	2	3	4	5	6	7	8	9
1	0.89	0	0	0	0	0	0	0	0
2	0	0.41	0.44	0	0	0	0	0	0
3	0	0	0	0.85	0	0	0	0	0.15
4	0	0.36	0	0	0	0	0	0	0
5	0.10	0	0	0	0	0	0	0	0
6	0	0	0	0	0	1.00	0	0	0
7	0	0	0	0	0	0	1.00	0	0
8	0	0	0	0	0.63	0	0	0	0
9	0	0	0	0	0	0	0	1.00	0
10	0	0	0	0	0.37	0	0	0	0

Supplemental Table 6. JI of UMAP between Monocle 3 (no Shuffle) and Cell/Gene-shuffled data1 (left) and data2 (right) of the *C.elegans*-con. The number inside the brackets is the average JI value for each comparison.

non-shuffle_vs_cell-shuffled 1 (0.92)

	1	2	3	4	5	6	7	8	9	10	11	12	13
1	0.97	0	0.01	0	0	0	0	0	0	0	0	0	0
2	0	0	0.74	0	0.23	0	0	0	0	0	0	0	0
3	0	0.93	0	0	0	0	0	0	0	0	0	0	0.06
4	0	0	0	0.99	0	0	0	0	0	0	0	0	0
5	0	0	0	0	0	0	0	0	0	0	0.61	0.38	0
6	0	0	0	0	0	0.98	0	0	0	0	0	0	0
7	0	0	0	0	0	0	0	0.98	0	0	0	0	0
8	0	0	0	0	0	0	0.97	0	0	0	0	0	0
9	0	0	0	0	0	0	0	0	1.00	0	0	0	0
10	0	0	0	0	0	0	0	0	0	0.99	0	0	0

non-shuffle_vs_cell-shuffled 2 (0.88)

	1	2	3	4	5	6	7	8	9	10	11	12	13	14
1	0.76	0.16	0	0	0	0	0	0	0	0	0	0	0	0
2	0	0.52	0	0	0	0.17	0	0	0	0	0	0.02	0.11	0
3	0	0	0.96	0	0	0	0	0	0	0	0	0	0	0.03
4	0	0	0	0.99	0	0	0	0	0	0	0	0	0	0
5	0	0	0	0	0	0	0	0	0	0	0.59	0.36	0	0
6	0	0	0	0	0.99	0	0	0	0	0	0	0	0	0
7	0	0	0	0	0	0	0	0.99	0	0	0	0	0	0
8	0	0	0	0	0	0	0.99	0	0	0	0	0	0	0
9	0	0	0	0	0	0	0	0	1.00	0	0	0	0	0
10	0	0	0	0	0	0	0	0	0	0.98	0	0	0	0

non-shuffle_vs_gene-shuffled 1 (0.74)

	1	2	3	4	5	6	7	8	9	10	11
1	0.81	0	0.01	0	0	0	0	0	0	0	0
2	0.12	0	0.41	0.15	0	0	0	0	0	0	0
3	0	0.81	0	0	0.10	0	0	0	0	0.03	0.02
4	0	0	0.31	0	0	0	0	0	0	0	0
5	0	0	0	0.55	0	0	0	0	0	0	0
6	0	0	0.01	0	0	0.95	0	0	0	0	0
7	0	0	0	0	0	0	0.99	0	0	0	0
8	0	0	0	0	0	0	0	0.99	0	0	0
9	0	0	0	0	0.57	0	0	0	0	0	0
10	0	0	0	0	0	0	0	0	0.99	0	0

non-shuffle_vs_gene-shuffled 2 (0.76)

	1	2	3	4	5	6	7	8	9	10	11
1	0.63	0.17	0	0	0	0	0	0	0	0	0
2	0.12	0.26	0	0.31	0	0	0	0	0	0	0
3	0	0	0.95	0	0	0	0	0	0	0	0.03
4	0	0.24	0	0	0	0	0	0	0	0	0
5	0	0	0	0.16	0	0	0	0	0	0.58	0
6	0	0.01	0	0	0.94	0	0	0	0	0	0
7	0	0	0	0	0	0.99	0	0	0	0	0
8	0	0	0	0	0	0	0.99	0	0	0	0
9	0	0	0	0	0	0	0	1.00	0	0	0
10	0	0	0	0	0	0	0	0	0.99	0	0

Supplemental Table 7. JI of t-SNE between Monocle 3 (no Shuffle) and Cell/Gene-shuffled data1 (left) and data2 (right) of the SCP345. The number inside the brackets is the average JI value for each comparison.

non-shuffle_vs_cell-shuffled 1 (0.96)

	1	2	3	4
1	0.96	0	0.02	0
2	0.01	0.98	0	0
3	0	0	0.91	0
4	0	0	0	1.00

non-shuffle_vs_cell-shuffled 2 (0.72)

	1	2	3	4	5	6
1	0.66	0	0	0.03	0	0
2	0.33	0	0	0	0	0.02
3	0	0.92	0	0	0.07	0
4	0	0	0.99	0	0	0

non-shuffle_vs_gene-shuffled 1 (0.96)

	1	2	3	4
1	0.98	0	0	0
2	0	0.98	0.01	0
3	0.01	0	0.9	0
4	0	0	0	1.00

non-shuffle_vs_gene-shuffled 2 (0.73)

	1	2	3	4
1	0.67	0	0	0
2	0.33	0	0	0
3	0	0.93	0	0.07
4	0	0	1.00	0

Supplemental Table 8. JI of UMAP between Monocle 3 (no Shuffle) and Cell/Gene-shuffled data1 (left) and data2 (right) of the SCP345. The number inside the brackets is the average JI value for each comparison.

non-shuffle_vs_cell-shuffled 1 (0.98)

	1	2	3	4	5	6
1	1.00	0	0	0	0	0
2	0	0.98	0	0	0	0
3	0	0	0.99	0	0	0
4	0	0	0	1.00	0	0
5	0	0	0	0	0.92	0
6	0	0	0	0	0	1.00

non-shuffle_vs_cell-shuffled 2 (0.98)

	1	2	3	4	5	6
1	0.99	0	0	0	0	0
2	0	0.98	0	0	0	0
3	0	0	0.99	0	0	0
4	0	0	0	1.00	0	0
5	0	0	0	0	0.92	0
6	0	0	0	0	0	0.99

non-shuffle_vs_gene-shuffled 1 (0.99)

	1	2	3	4	5	6
1	1.00	0	0	0	0	0
2	0	0.99	0	0	0	0
3	0	0	0.99	0	0	0
4	0	0	0	1.00	0	0
5	0	0	0	0	0.98	0
6	0	0	0	0	0	1.00

non-shuffle_vs_gene-shuffled 2 (0.98)

	1	2	3	4	5	6
1	0.99	0	0	0	0	0
2	0	0.98	0	0	0	0
3	0	0	0.99	0	0	0
4	0	0	0	1.00	0	0
5	0	0	0	0	0.98	0
6	0	0	0	0	0	0.97

Supplemental Table 9. JI of t-SNE between Monocle 3 (no Shuffle) and Cell/Gene-shuffled data1 (left) and data2 (right) of the SCP1526. The number inside the brackets is the average JI value for each comparison.

non-shuffle_vs_cell-shuffled 1 (0.72)

	1	2	3	4	5	6	7	8	9	10	11	12	13
1	0.70	0.01	0.04	0	0	0	0	0	0	0	0.01	0	0
2	0	0.02	0.81	0	0	0.07	0	0	0	0	0	0	0
3	0	0.09	0	0.79	0	0	0	0	0	0	0	0	0
4	0	0.63	0	0	0	0	0	0	0	0	0	0	0
5	0.22	0.11	0	0	0	0	0	0	0	0	0	0	0
6	0.01	0	0	0.01	0.95	0	0	0	0	0	0	0	0
7	0	0	0.01	0	0	0.38	0	0	0.36	0	0	0	0
8	0	0	0	0	0	0	0.99	0	0	0	0	0	0
9	0	0	0	0	0	0	0	1.00	0	0	0	0	0
10	0	0	0	0	0	0	0	0	0	0.99	0	0	0
11	0	0	0	0.02	0	0	0	0	0	0	0	0	0
12	0	0	0	0	0	0	0.01	0	0	0	0	0.92	0
13	0	0	0	0	0	0	0	0	0	0	0	0	0.96

non-shuffle_vs_cell-shuffled 2 (0.73)

	1	2	3	4	5	6	7	8	9	10	11	12	13
1	0.91	0.02	0	0	0	0.01	0	0	0	0	0	0.01	0
2	0.01	0.89	0	0.01	0.02	0	0	0	0	0	0	0	0
3	0	0	0.76	0.09	0.01	0	0	0	0	0	0	0	0
4	0	0	0	0.78	0	0	0	0	0	0	0	0	0
5	0	0	0.04	0	0.77	0.02	0	0	0	0	0	0	0
6	0	0	0	0.01	0	0.88	0	0	0	0	0	0	0
7	0	0	0	0	0	0	0	0	0.62	0.35	0	0	0
8	0	0	0	0	0	0	1.00	0	0	0	0	0	0
9	0	0	0	0	0	0	0	1.00	0	0	0	0	0
10	0	0	0	0	0	0	0	0	0	0	0.62	0	0
11	0	0	0.02	0	0	0	0	0	0	0	0	0	0
12	0	0	0	0	0	0	0	0	0	0	0.38	0	0
13	0	0	0	0	0	0	0	0	0	0	0	0	0.90

non-shuffle_vs_gene-shuffled 1 (0.76)

	1	2	3	4	5	6	7	8	9	10	11	12
1	0.7	0	0	0.01	0.01	0	0	0	0	0.01	0	0
2	0	0	0.98	0	0	0	0	0	0	0	0	0
3	0	0.96	0	0	0	0	0	0	0	0	0.01	0
4	0	0	0	0.95	0	0	0	0	0	0	0	0
5	0	0	0	0	0.96	0	0	0	0	0	0	0
6	0.28	0	0	0	0	0	0	0	0	0	0	0
7	0	0	0	0	0	1.00	0	0	0	0	0	0
8	0	0	0	0	0	0	1.00	0	0	0	0	0
9	0	0	0	0	0	0	0	1.00	0	0	0	0
10	0	0	0	0	0	0	0	0	0.62	0	0	0
11	0	0.01	0	0	0	0	0	0	0	0	0	0
12	0	0	0	0	0	0	0	0	0.38	0	0	0
13	0	0	0	0	0	0	0	0	0	0	0	1.00

non-shuffle_vs_gene-shuffled 2 (0.90)

	1	2	3	4	5	6	7	8	9	10	11	12	13
1	0.71	0	0	0	0.01	0	0	0	0	0	0.01	0	0
2	0	0.96	0	0.01	0	0	0	0	0	0	0	0	0
3	0	0	0.96	0	0.02	0	0	0	0	0	0	0	0
4	0	0	0	0.96	0	0	0	0	0	0	0	0	0
5	0	0	0	0	0.92	0	0	0	0	0	0	0	0
6	0.27	0	0	0	0	0	0	0	0	0	0	0	0
7	0	0	0	0	0	0.99	0	0	0	0	0	0	0
8	0	0	0	0	0	0	1.00	0	0	0	0	0	0
9	0	0	0	0	0	0	0	1.00	0	0	0	0	0
10	0	0	0	0	0	0	0	0	0.99	0	0	0	0
11	0	0	0	0	0	0	0	0	0	1.00	0	0	0
12	0	0	0	0	0	0	0	0	0	0	0	0.99	0
13	0	0	0	0	0	0	0	0	0	0	0	0	1.00

Supplemental Table 10. JI of UMAP between Monocle 3 (no Shuffle) and Cell/Gene-shuffled data1 (left) and data2 (right) of the SCP1526. The number inside the brackets is the average JI value for each comparison.

non-shuffle_vs_cell-shuffled 1 (0.85)

	1	2	3	4	5	6	7	8	9	10	11	12
1	0.91	0.01	0	0	0	0	0	0	0	0	0	0
2	0	0.95	0	0	0	0	0	0	0	0	0	0
3	0	0	0.97	0	0	0	0	0	0	0	0	0
4	0	0	0	0.97	0.01	0	0	0	0	0	0	0
5	0	0	0	0	0.95	0.01	0	0	0	0	0	0
6	0	0.01	0	0	0	0.92	0	0	0	0	0.02	0
7	0	0	0	0	0	0	0.99	0	0	0	0	0
8	0	0	0	0	0	0	0	0.92	0	0.07	0	0
9	0	0	0	0	0	0	0	0	1.00	0	0	0
10	0.06	0	0	0	0	0	0	0	0	0	0	0
11	0	0	0	0	0	0	0	0	0	0.62	0	0
12	0	0	0	0	0	0	0	0	0	0	0	0.90

non-shuffle_vs_cell-shuffled 2 (0.86)

	1	2	3	4	5	6	7	8	9	10	11	12	13
1	0.97	0	0	0	0	0	0	0	0	0	0	0	0
2	0	0.96	0	0	0	0	0	0	0	0	0	0	0
3	0	0	0.97	0	0	0	0	0	0	0	0	0	0
4	0	0	0.01	0.97	0.01	0	0	0	0	0	0	0	0
5	0	0	0	0	0.96	0	0	0	0	0	0	0	0
6	0	0.01	0	0	0	0.93	0	0	0	0	0	0.02	0
7	0	0	0	0	0	0	0	0	0.60	0	0.37	0	0
8	0	0	0	0	0	0	0.89	0	0	0	0	0	0
9	0	0	0	0	0	0	0	1.00	0	0	0	0	0
10	0	0	0	0	0	0	0	0	0	0.97	0	0	0
11	0	0	0	0	0	0	0.11	0	0	0	0	0	0
12	0	0	0	0	0	0	0	0	0	0	0	0	0.93

non-shuffle_vs_gene-shuffled 1 (0.85)

	1	2	3	4	5	6	7	8	9	10	11	12
1	0.10	0.74	0	0	0	0	0	0	0	0	0	0
2	0.81	0	0	0	0	0	0	0	0	0	0	0
3	0	0	0.97	0	0	0	0	0	0	0	0	0
4	0	0	0.01	0.97	0	0	0	0	0	0	0	0
5	0	0	0	0	0.94	0	0	0	0	0	0	0
6	0.01	0	0	0	0.01	0.93	0	0	0	0	0	0
7	0	0	0	0	0	0	0.95	0	0	0	0	0
8	0	0	0	0	0	0	0	0.92	0	0	0.08	0
9	0	0	0	0	0	0	0	0	1.00	0	0	0
10	0	0.07	0	0	0	0	0	0	0	0	0	0
11	0	0	0	0	0	0	0	0	0	0.99	0	0
12	0	0	0	0	0	0	0	0	0	0	0	0.89

non-shuffle_vs_gene-shuffled 2 (0.68)

	1	2	3	4	5	6	7	8	9	10	11
1	0	0.90	0	0	0	0	0	0	0	0	0
2	0	0.01	0.96	0	0	0	0	0	0	0	0
3	0.50	0	0	0	0	0	0	0	0	0	0
4	0.48	0	0	0	0	0	0	0	0	0	0
5	0	0	0	0.73	0	0	0	0	0	0	0
6	0	0	0	0.16	0.62	0	0	0	0	0.02	0
7	0	0	0	0	0	0.97	0	0	0	0	0
8	0	0	0	0	0	0	0.92	0	0	0	0.08
9	0	0	0	0	0	0	0	1.00	0	0	0
10	0	0.06	0	0	0	0	0	0	0	0	0
11	0	0	0	0	0	0	0	0	0.99	0	0
12	0	0	0	0.01	0	0	0	0	0	0	0

Supplemental Table 11. JI of t-SNE between Monocle 3 (no Shuffle) and Cell/Gene-shuffled data1 (left) and data2 (right) of the Mouse Retina. The number inside the brackets is the average JI value for each comparison.

non-shuffle_vs_cell-shuffled 1 (0.98)

	1	2	3	4	5	6	7	8	9	10
1	0.93	0	0	0	0.07	0	0	0	0	0
2	0	0.99	0	0	0	0	0	0	0	0
3	0	0	1.00	0	0	0	0	0	0	0
4	0	0	0	1.00	0	0	0	0	0	0
5	0	0	0	0	0	0.90	0	0	0	0.09
6	0	0	0	0	0	0	0.98	0	0	0
7	0	0	0	0	0	0	0	1.00	0	0
8	0	0	0	0	0	0	0	0	1.00	0

non-shuffle_vs_cell-shuffled 2 (0.73)

	1	2	3	4	5	6	7	8	9
1	1.00	0	0	0	0	0	0	0	0
2	0	0.99	0	0	0	0	0	0	0
3	0	0	0.42	0	0.25	0	0	0	0
4	0	0	0	1.00	0	0	0	0	0
5	0	0	0.32	0	0	0.22	0	0	0.09
6	0	0	0.14	0	0	0	0	0	0
7	0	0	0	0	0	0	1.00	0	0
8	0	0	0	0	0	0	0	1.00	0

non-shuffle_vs_gene-shuffled 1(1.00)

	1	2	3	4	5	6	7	8
1	1.00	0	0	0	0	0	0	0
2	0	1.00	0	0	0	0	0	0
3	0	0	1.00	0	0	0	0	0
4	0	0	0	1.00	0	0	0	0
5	0	0	0	0	0.99	0	0	0
6	0	0	0	0	0	1.00	0	0
7	0	0	0	0	0	0	1.00	0
8	0	0	0	0	0	0	0	1.00

non-shuffle_vs_gene-shuffled 2 (0.87)

	1	2	3	4	5	6	7
1	0.99	0	0	0	0	0	0
2	0	0	1.00	0	0	0	0
3	0	0.57	0	0	0	0	0
4	0	0	0	1.00	0	0	0
5	0.01	0.41	0	0	0	0	0
6	0	0	0	0	1.0(	0	0
7	0	0	0	0	0	1.00	0
8	0	0	0	0	0	0	1.00

Supplemental Table 12. JI of UMAP between Monocle 3 (no Shuffle) and Cell/Gene-shuffled data1 (left) and data2 (right) of the Mouse Retina. The number inside the brackets is the average JI value for each comparison.

non-shuffle_vs_cell-shuffled 1(0.78)

	1	2	3	4	5	6	7	8	9	10
1	0.99	0	0	0	0	0	0	0	0	0
2	0	0.99	0	0	0	0	0	0	0	0
3	0	0	0	0.99	0	0	0	0	0	0
4	0	0	0	0	0	0.99	0	0	0	0
5	0	0	0	0	0	0	0.99	0	0	0
6	0	0	0	0	0.82	0	0	0	0	0
7	0	0	0.72	0	0	0	0	0	0.01	0
8	0	0	0.06	0	0	0	0	0.63	0	0
9	0	0	0.2	0	0	0	0	0	0	0
10	0	0	0	0	0.15	0	0	0	0	0
11	0	0	0	0	0	0	0	0	0.92	0
12	0	0	0	0	0	0	0	0	0	1.00

non-shuffle_vs_cell-shuffled 2(0.82)

	1	2	3	4	5	6	7	8	9	10
1	1.00	0	0	0	0	0	0	0	0	0
2	0	1.00	0	0	0	0	0	0	0	0
3	0	0	0	0	0.99	0	0	0	0	0
4	0	0	0	0	0	0.99	0	0	0.01	0
5	0	0	0	0	0	0	0.99	0	0	0
6	0	0	0	0.83	0	0	0	0	0	0
7	0	0	0.77	0	0	0	0	0	0.01	0
8	0	0	0	0	0	0	0	0.97	0	0
9	0	0	0.22	0	0	0	0	0	0	0
10	0	0	0	0.14	0	0	0	0	0	0
11	0	0	0	0	0	0	0	0	0.92	0
12	0	0	0	0	0	0	0	0	0	1.00

non-shuffle_vs_gene-shuffled 1(0.85)

	1	2	3	4	5	6	7	8	9	10	11	12	13
1	1.00	0	0	0	0	0	0	0	0	0	0	0	0
2	0	0.99	0	0	0	0	0	0	0	0	0	0	0
3	0	0	0	0.99	0	0	0	0	0	0	0	0	0
4	0	0	0	0	0	0	0.63	0.35	0	0	0	0	0
5	0	0	0	0	0.99	0	0	0	0	0	0	0	0
6	0	0	0	0	0	0.98	0	0	0	0	0	0	0
7	0	0	0.77	0	0	0	0	0	0	0	0	0	0
8	0	0	0	0	0	0	0	0	0.63	0	0	0.33	0
9	0	0	0.22	0	0	0	0	0	0	0	0	0	0
10	0	0	0	0	0	0	0	0	0	0.98	0	0	0
11	0	0	0	0	0	0	0	0	0	0	1.00	0	0
12	0	0	0	0	0	0	0	0	0	0	0	0	1.00

non-shuffle_vs_gene-shuffled 2 (0.87)

	1	2	3	4	5	6	7	8	9	10	11	12	13
1	1.00	0	0	0	0	0	0	0	0	0	0	0	0
2	0	0.99	0	0	0	0	0	0	0	0	0	0	0
3	0	0	0	0.99	0	0	0	0	0	0	0	0	0
4	0	0	0	0	0	0	0.88	0	0	0	0.12	0	0
5	0	0	0	0	0.99	0	0	0	0	0	0	0	0
6	0	0	0	0	0	0.98	0	0	0	0	0	0	0
7	0	0	0.78	0	0	0	0	0	0	0	0	0	0
8	0	0	0	0	0	0	0	0.63	0	0	0	0.35	0
9	0	0	0.22	0	0	0	0	0	0	0	0	0	0
10	0	0	0	0	0	0	0	0	0.97	0	0	0	0
11	0	0	0	0	0	0	0	0	0	1.00	0	0	0
12	0	0	0	0	0	0	0	0	0	0	0	0	1.00

Supplemental Table 13. JI of t-SNE between Monocle 3 (no Shuffle) and Cell/Gene-shuffled data1 (left) and data2 (right) of the Mouse Brain. The number inside the brackets is the average JI value for each comparison.

non-shuffle_vs_cell-shuffled 1(0.74)

	1	2	3	4	5	6	7	8	9	10
1	1.00	0	0	0	0	0	0	0	0	0
2	0	0.32	0.58	0	0	0	0	0	0	0
3	0	0.29	0	0	0	0.54	0	0	0	0
4	0	0	0	1.00	0	0	0	0	0	0
5	0	0	0	0	0	0	1.00	0	0	0
6	0	0	0	0	0.51	0	0	0	0	0
7	0	0	0	0	0.25	0	0	0	0	0
8	0	0	0	0	0	0	0	1.00	0	0
9	0	0	0	0	0.23	0	0	0	0	0
10	0	0	0	0	0	0	0	0	1.00	0
11	0	0	0	0	0	0	0	0	0	1.00

non-shuffle_vs_cell-shuffled 2(0.68)

	1	2	3	4	5	6	7	8	9
1	1.00	0	0	0	0	0	0	0	0
2	0	0.99	0	0	0	0	0	0	0
3	0	0.01	0	0	0.54	0.44	0	0	0
4	0	0	0	1.00	0	0	0	0	0
5	0	0	0	0	0	0	1.00	0	0
6	0	0	0.46	0	0	0	0	0	0
7	0	0	0.23	0	0	0	0	0	0
8	0	0	0	0	0	0	0	1.00	0
9	0	0	0.21	0	0	0	0	0	0
10	0	0	0.1	0	0	0	0	0	0
11	0	0	0	0	0	0	0	0	1.00

non-shuffle_vs_gene-shuffled 1 (1.00)

	1	2	3	4	5	6	7	8	9
1	1.00	0	0	0	0	0	0	0	0
2	0	1.00	0	0	0	0	0	0	0
3	0	0	1.00	0	0	0	0	0	0
4	0	0	0	1.00	0	0	0	0	0
5	0	0	0	0	1.00	0	0	0	0
6	0	0	0	0	0	1.00	0	0	0
7	0	0	0	0	0	0	1.00	0	0
8	0	0	0	0	0	0	0	1.00	0
9	0	0	0	0	0	0	0	0	1.00

non-shuffle_vs_gene-shuffled 2 (1.00)

	1	2	3	4	5	6	7	8	9
1	1.00	0	0	0	0	0	0	0	0
2	0	1.00	0	0	0	0	0	0	0
3	0	0	1.00	0	0	0	0	0	0
4	0	0	0	1.00	0	0	0	0	0
5	0	0	0	0	1.00	0	0	0	0
6	0	0	0	0	0	1.00	0	0	0
7	0	0	0	0	0	0	1.00	0	0
8	0	0	0	0	0	0	0	1.00	0
9	0	0	0	0	0	0	0	0	1.00

Supplemental Table 14. JI of UMAP between Monocle 3 (no Shuffle) and Cell/Gene-shuffled data1 (left) and data2 (right) of the Mouse Brain. The number inside the brackets is the average JI value for each comparison.

non-shuffle_vs_cell-shuffled 1 (0.97)

	1	2	3	4	5	6	7	8	9	10
1	1.00	0	0	0	0	0	0	0	0	0
2	0	1.00	0	0	0	0	0	0	0	0
3	0	0	0.99	0	0	0	0	0	0	0
4	0	0	0	1.00	0	0	0	0	0	0
5	0	0	0	0	0	0	0.90	0	0	0
6	0	0	0	0	1.00	0	0	0	0	0
7	0	0	0	0	0	1.00	0	0	0	0
8	0	0	0	0	0	0	0	0.99	0	0
9	0	0	0	0	0	0	0	0	0.71	0
10	0	0	0	0	0	0	0	0	0	1.00

non-shuffle_vs_cell-shuffled 2 (0.98)

	1	2	3	4	5	6	7	8	9	10
1	1.00	0	0	0	0	0	0	0	0	0
2	0	0	0.70	0	0	0	0	0	0	0.30
3	0	1.00	0	0	0	0	0	0	0	0
4	0	0	0	1.00	0	0	0	0	0	0
5	0	0	0	0	1.00	0	0	0	0	0
6	0	0	0	0	0	1.00	0	0	0	0
7	0	0	0	0	0	0	1.00	0	0	0
8	0	0	0	0	0	0	0	0.99	0	0
9	0	0	0	0	0	0	0	0	1.00	0
10	0	0	0	0	0	0	0	0	0	0

non-shuffle_vs_gene-shuffled 1(0.96)

	1	2	3	4	5	6	7	8	9	10
1	1.00	0	0	0	0	0	0	0	0	0
2	0	0	0.68	0	0	0	0	0	0	0.31
3	0	0.95	0	0	0	0	0	0	0	0
4	0	0	0	1.00	0	0	0	0	0	0
5	0	0	0	0	1.00	0	0	0	0	0
6	0	0	0	0	0	1.00	0	0	0	0
7	0	0	0	0	0	0	1.00	0	0	0
8	0	0	0	0	0	0	0	0.99	0	0
9	0	0	0	0	0	0	0	0	1.00	0
10	0	0	0	0	0	0	0	0	0	0

non-shuffle_vs_gene-shuffled 2(0.96)

	1	2	3	4	5	6	7	8	9	10
1	1.00	0	0	0	0	0	0	0	0	0
2	0	1.00	0	0	0	0	0	0	0	0
3	0	0	0.96	0	0	0	0	0	0	0
4	0	0	0	1.00	0	0	0	0	0	0
5	0	0	0	0	1.00	0	0	0	0	0
6	0	0	0	0	0	1.00	0	0	0	0
7	0	0	0	0	0	0	1.00	0	0	0
8	0	0	0	0	0	0	0	1.00	0	0
9	0	0	0	0	0	0	0	0	0.70	0
10	0	0	0	0	0	0	0	0	0	1.00